THE ABILITIES & INABILITIES OF WOUND ROLL MODELS TO PREDICT WINDING DEFECTS

by

J. K. Good
Oklahoma State University
USA

ABSTRACT

Wound roll models began appearing in the literature 40 years ago. These models predict internal stresses within wound rolls due to winder operating conditions and web material properties. The models have progressed much in their ability to model the complex properties of webs and winder type on the internal stresses. Defect models have also advanced but not at the rate of the wound roll models. The first objective of this paper is to establish the current state of wound roll and winding defect models that can be used to enhance productivity in web process machinery. The second objective is to establish what winding defects cannot be attacked with current models and why.

INTRODUCTION

There are several types of winders which are in present use. Web materials which are vastly diverse are wound on these machines. These webs experience various defects as a result of being wound. The types of defects that result are the combined result of stresses induced in the web by winding and the web material properties. Often rolls of web material may set in storage for a period of time prior to conversion to a final product. While in storage the web may experience inelastic deformation which may be affected by environmental factors. Rolls which appeared to be of good quality at the time of winding may exhibit defects after storage.

Winding models appeared in the literature over 40 years ago which provided the first insight of how the internal stresses vary within the wound roll. Some of the largest handling related losses in web process lines occur at the winder or while wound rolls are in storage. Very few sources have appeared in which winding defects have been eliminated or production has been increased through the use of wound roll models. A partial explanation may be that in a competitive environment the public discussion of methods in which waste has been decreased and production increased may not be condoned. Another explanation could be that the winding defects encountered were resolved by winding trials in which the winder inputs were varied until the defect was

eliminated. These trials can be costly, especially when they must be performed on a production winder. In many cases there is the potential for multiple types of defects in winding rolls. A decrease in winding tension may prevent a blocking defect from occurring while winding but now there may be insufficient pressure in the roll such that it can be transported or unwound without damage. There may be but small windows of opportunity in the winder control parameters that will produce defect free rolls that can be unwound with acceptable loss. It is in such cases where wound roll and winding defect models become more efficient than the trial method of eliminating winding defects.

The purpose of this paper is to generate an awareness of winding models and what defects one can hope to resolve using these models. Models will never entirely replace winding trials, winder operators can sometimes eliminate defects through trial and error winding faster than a model could be run to aid the decision process. Winding models can be helpful in solving defect problems. Models can be used to forecast the impact of web material, coating modifications or process line changes such as changes in process temperature or perhaps an increase in web velocity. The models can also be helpful when selecting winding equipment.

WINDING MODELS

Winding Models in One Dimension

A good number of references have focused on winding models. The majority of these models are one-dimensional and allow one to predict how the stresses within the wound roll behave as a function of radius. All of these models begin with an assumption that the spiral form of the wound roll can be represented as a series of concentric accreted hoops of web. These efforts have advanced the understanding of how internal stresses vary in wound rolls. Most of these models rely upon the equilibrium equation written in cylindrical coordinates:

$$r\frac{d\sigma_r}{dr} + \sigma_r - \sigma_\theta = 0 \qquad \{1\}$$

Next constitutive equations are developed which relate strain to stress. Choices must then be made to determine if the roll being wound is in a state of plane stress or plane strain.

Plane Stress Models. The majority of the models developed incorporate the assumption of plane stress conditions where the following constitutive relations apply:

$$\varepsilon_r = \frac{\sigma_r}{E_r} - \frac{\nu_{r\theta}\sigma_\theta}{E_\theta}$$
$$\varepsilon_\theta = \frac{\sigma_\theta}{E_\theta} - \frac{\nu_{\theta r}\sigma_r}{E_r} \qquad \{2\}$$

E_r and E_θ are the radial and tangential Young's moduli, respectively, and $\nu_{r\theta}$ is Poisson's ratio relating the impact of a stress in the θ-direction to the strain in the r-direction. In plane stress, the stress in the z or CMD direction is assumed to be zero. At this point the models begin to differ. Early models, Gutterman [1] and Catlow et al. [2], assumed that a wound roll could be modeled as a linear isotropic material, where the radial modulus was equivalent to the circumferential modulus of elasticity (E_r=E_θ). The next generation of models, Altmann [3] and Yagoda [4], assumed the wound roll could be modeled as a linear anisotropic material, where E_r was unequal to E_θ although both parameters are assumed to be constants. One of the benefits of assuming E_r and E_θ to be constants is that

a reverse model can be posed. Thus if it known prior to winding that a certain profile in radial pressure is desirable for a given web, the reverse model would allow one to solve for the profile in winding tension as a function of wound roll radius that would yield that profile in radial pressure[5].

In reality the radial modulus of a wound roll is a state dependent parameter which encompasses both structural and material nonlinearities. Paper, plastic film, metal foils and other webs have asperities upon their surfaces and when the web is wound or stacked asperities from one surface contact asperities upon the next surface. Some webs like paper and non-wovens have internal nonlinearities throughout the sheet thickness in compression. Thus upon compression the surface and sometimes the internal contact area becomes a function of radial or normal pressure and the measured radial modulus, E_r, is a function of radial stress. Typically the sign convention for stress is one in which tensile stresses are positive and hence compressive stresses are negative. Tensile radial stresses in a wound roll have no physical meaning since this would result in separation of layers. Hence it is often convenient to replace the radial stress (σ_r) with pressure (P) simply by omission of the sign. Since E_r is state dependent there are a number of empirical forms which have been used to relate E_r to pressure. Pfeiffer [6] noted that the relation between the normal pressure and the normal strain appeared logarithmic in the form:

$$P = -\sigma_r = K_1\left(e^{K_2\varepsilon_r} - 1\right) \qquad \{3\}$$

The modulus is therefore:

$$E_r = \frac{dP}{d\varepsilon_r} = K_2\left(P + K_1\right) \qquad \{4\}$$

and thus the dependency of modulus upon pressure is limited to a linear relationship. Results from stack compression tests sometimes indicate that a higher order polynomial is required to provide a satisfactory correlation to the data. Hakiel [7] allowed the radial modulus to vary as a polynomial in pressure:

$$E_r = C_1 + C_2P + C_3P^2 + \ldots \qquad \{5\}$$

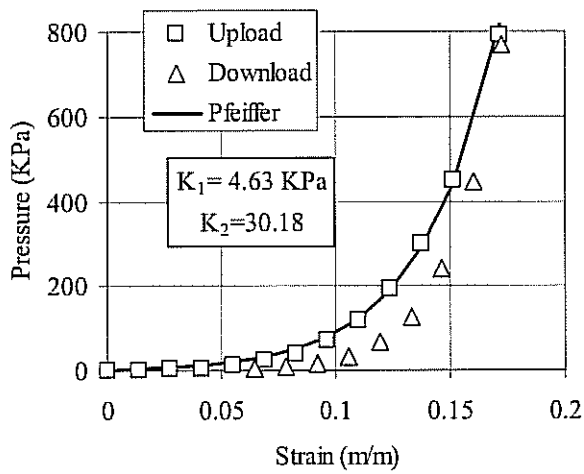

Figure 1 – A Stack Compression Test Performed on Polyester Displaying Typical Hysteresis and the Ability of Pfeiffer's Form (3) to Fit the Data.

The constants C_n must be determined experimentally and if limited to the constants C_1 and C_2 is equivalent to Pfeiffer's form. Pfeiffer's form is convenient in that once K_1 and K_2 are determined one has both a relationship for pressure versus strain in expression {3} and modulus versus pressure in expression {4}. Results of stack tests are indicative of hysteresis between the pressure associated with a given strain on upload and download. Such results are shown for a polyester web in Figure 1. Winding is an upload phenomena; it is typical for the pressures at all radii to increase monotonically or to increase to a maximum pressure asymptotically during winding. Thus in winding models the radial modulus associated with an upload in a stack test should be employed. Typical values for the material properties of several paper types are given in Table 1.

Paper Type	thickness (μm)	E_θ (GPa)	K_1 (KPa)	K_2
Light Weight Coated	44.5	5.54	1.34	59.7
Newsprint	71.1	4.02	0.69	27.5
Fine Coated Paper	88.9	6.27	2.74	182.6
Supercalendared	96.5	7.90	3.18	35.6

Table 1 – Typical Paper Properties.

Willett and Poesch [8] allow the radial strain to be related to a polynomial in stress, very similar to that of Hakiel [7]. They also attempted to measure the Poisson's ratio $\nu_{\theta r}$ in stack compression tests. It was assumed that the tangential stress σ_θ was nil and insertion of this assumption into the constitutive equations {2} allows the conclusion:

$$\nu_{\theta r} = -\frac{\varepsilon_r}{\varepsilon_\theta} \qquad \{6\}$$

The radial strain in the stack is easily measured in a compression test, however the tangential strain measurement has proven a significant challenge. Willett and Poesch attempted this by developing an optical laser interference method to measure the lateral expansion of stack subject to compression. Willett and Poesch reported an average value of $\nu_{\theta r}$ to be 0.07. Both Hakiel [7] and Willett and Poesch [8] present the argument that based upon strain energy density that the coefficients in the constitutive equations {2} must be symmetric or:

$$\frac{\nu_{r\theta}}{E_\theta} = \frac{\nu_{\theta r}}{E_r} \qquad \{7\}$$

This expression is sometimes referred to as Maxwell's equation. For many paper, plastic, and foil webs the in-plane modulus E_θ is constant and the radial modulus E_r is state dependent on the radial stress σ_r. If Maxwell's expression is valid for web layers in compression at least one and maybe both Poisson's ratios must also be state dependent. It should also be stated that expression {7} has never been experimentally validated but nor has it been proven invalid for stacks. Benson [9] argues that expression {7} need not be used in model development but also that the point is moot as the Poisson's ratios are known to be small. Use of wound roll models also indicates the impact of varying the input Poisson's ratios are small on the internal stresses produced within the wound roll. Good and Markum conducted stack compression tests on polyester films that verify that $\nu_{\theta r}$ is state dependent on pressure. In these tests, strain gages where adhered to the film surface in the tangential direction (ε_θ). The strain in the normal or r direction (ε_r) in the stack was measured and controlled during the test. Using the two measured strains the Poisson's ratio $\nu_{\theta r}$ could be inferred using expression {6} at various pressure levels on the stack. Results of these tests are shown in Figure 2.

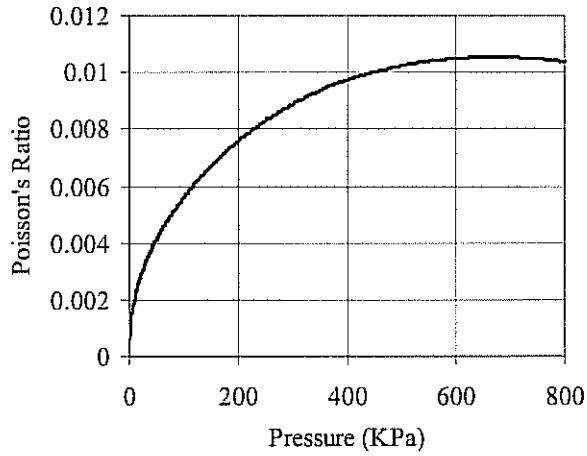

Figure 2 – The State Dependency of Poisson's Ratio ($\nu_{\theta r}$) on Pressure.

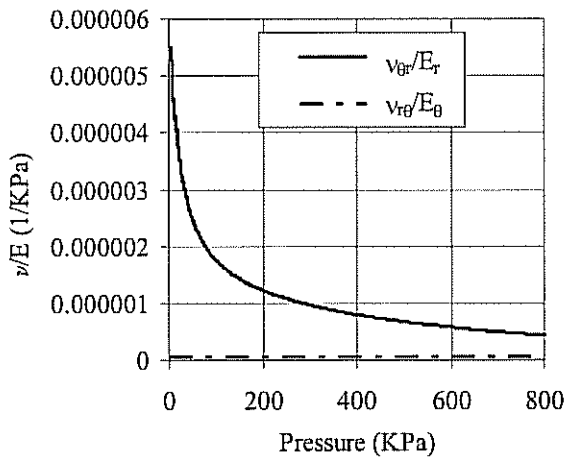

Figure 3 – Is Maxwell's Expression {7} is Valid for Stacks?

In Figure 2 it appears $\nu_{\theta r}$ is dependent on radial stress but approaches a constant value close to 0.01, a value Hakiel employed [7]. The Poisson ratio $\nu_{r\theta}$ is assumed constant for film webs and in the range of 0.3-0.4, this Poisson ratio would govern the thinning of the web in the r direction when subjected to tension in the tangential direction. When the right hand side of equation {7} is developed it remains a function of pressure and significantly different from the constant value resulting in the left hand side of the expression, note Figure 3. Thus it appears opportune that the models are not greatly affected by the values of Poisson's ratio. The two ratios in Maxwell's expression {7} do appear to approach one another at higher pressures.

In cylindrical coordinates, the symmetric components of linear strain are:

$$\varepsilon_r = \frac{du}{dr} \quad \text{and} \quad \varepsilon_\theta = \frac{u}{r} \qquad \{8\}$$

where u is the symmetric radial deformation and a function of radius. If the radial deformation is eliminated from these strain relations a compatibility expression between

the two strains can be established which dictates how the two strains are related at all radial locations:

$$\varepsilon_\theta - \varepsilon_r + \frac{d\varepsilon_\theta}{dr} r = 0 \qquad \{9\}$$

Hakiel [7] combined equilibrium {1}, compatibility {9}, and material relationships {2,7} to yield a second order differential equation in radial pressure with a non-constant coefficient in E_r :

$$r^2 \frac{d^2\sigma_r}{dr^2} + 3r\frac{d\sigma_r}{dr} - \left(\frac{E_\theta}{E_r} - 1\right)\sigma_r = 0 \qquad \{10\}$$

Since the equation is second order, two boundary conditions are required which are related to σ_r. The wound roll is an accretive structure and as layers are added the boundary conditions may change and the radial modulus may be changing as a function of the pressures at various radii. Equation {10} must be solved many times, in extreme cases as many times as there are layers in the roll. Thus instead of solving for the total pressure σ_r, one solves for increments in pressure $\delta\sigma_r$ due to the addition of the last layer(s). Expression {10} becomes:

$$r^2 \frac{d^2\delta\sigma_r}{dr^2} + 3r\frac{d\delta\sigma_r}{dr} - \left(\frac{E_\theta}{E_r} - 1\right)\delta\sigma_r = 0 \qquad \{11\}$$

The boundary conditions must be written then in terms of these incremental pressures. The first boundary condition assumes the tension (T_w, in units of stress) in the outer lap (at radius r=s) is known and employs the hoop stress relation which was derived to relate the internal pressure within thin wall pressure vessels to the tangential stress:

$$\delta\sigma_r\Big|_{r=s} = -\frac{T_w\big|_{r=s}}{s} h \qquad \{12\}$$

where h is the thickness of the layer and the sign results from pressure being defined as a negative stress. Thus the first boundary condition results from knowledge of the pressure level beneath the most recent lap that was accreted. The second boundary condition is based upon displacement compatibility between the first layer of the wound roll and the core which it is in contact with. Hakiel normalized the radial deformations by dividing by the outside radius of the core and wrote this boundary condition as:

$$\frac{u}{r_c} = u\Big|_{r=r_c} = \frac{\delta\sigma_r\big|_{r=r_c}}{E_c} \qquad \{13\}$$

where E_c is the core stiffness and u is the deformation of the outside of the core normalized by the outer radius of the core (r_c). The strain, or equivalently the normalized deformation in the first layer of web, can be written then as:

$$\varepsilon_\theta = \frac{u}{r_c} = u\big|_{r=layer1} = \frac{\delta\sigma_\theta}{E_\theta} - \frac{\nu_{\theta r}\delta\sigma_r}{E_r} = \frac{1}{E_\theta}\left(\delta\sigma_\theta - \nu_{r\theta}\delta\sigma_r\right)\Big|_{r=layer1} \qquad \{14\}$$

Equating the normalized deformations of {13} and {14} and employing the equilibrium expression {1} allows the second boundary condition to be written as:

$$\frac{d\delta\sigma_r}{dr}\Big|_{r=1} = \left(\frac{E_\theta}{E_c} - 1 + \nu_{r\theta}\right)\frac{\delta\sigma_r}{r_c}\Big|_{r=1} \qquad \{15\}$$

Equation {11} is then solved using the boundary conditions of {12} and {15} yielding the increments in pressure throughout the roll due to the addition of the last lap. After the

addition of each lap the increments in pressure are summed with all previous increments in pressure within each layer to provide the total pressure as a function of radius throughout the roll. Thus the total radial stress in the i^{th} lap through the addition of all laps outboard will be:

$$\sigma_{ri} = \sum_{j=i+1}^{n} \delta\sigma_{rij} \qquad \{16\}$$

With the radial stress known within each lap and thus as a function of radius, the derivative of the radial stress can be estimated and the equilibrium expression {1} can be used to determine the tangential stress as a function of radius:

$$\sigma_\theta = r\frac{d\sigma_r}{dr} + \sigma_r \qquad \{17\}$$

Hakiel's derivation is focused upon here as it was the first complete model that accounted for core deformation and the state dependency that Pfeiffer found in the radial modulus. Hakiel verified his model through center winding tests of paper and plastic films and found it adequately predicted the internal pressure in those rolls. Other authors have developed models based upon strain and energy methods but none have been proven more accurate than Hakiel's model [10-14]. Thus Hakiel's contribution was key in the development of wound roll models.

There are generally two types of behavior, radial stress as a function of radius, that can result from these models. Struik [15] categorized these behaviors as *spongy* and *fully compressed*. These behaviors result from the value of the ratio of E_θ/E_r in expression {11}. As E_r approaches E_θ the material behavior approaches isotrophy and results in a *fully compressed* behavior in which the radial stress decays monotonically from the core to the outer wound roll radius when winding at constant tension. In cases in which E_r is much less than E_θ the radial stress may be nearly independent of radius except in the vicinity of the core and the outermost layers which is the *spongy* behavior. A given web material may exhibit both behaviors depending on the winding tension which in turn affects the radial stress and the radial modulus. As an example a winding model of the type described by Hakiel was used to study center winding of a fine coated paper whose properties were listed in Table 1. This web was wound upon an aluminum core for which the inside and outside radius were 3.8 and 5.1 cm, respectively.

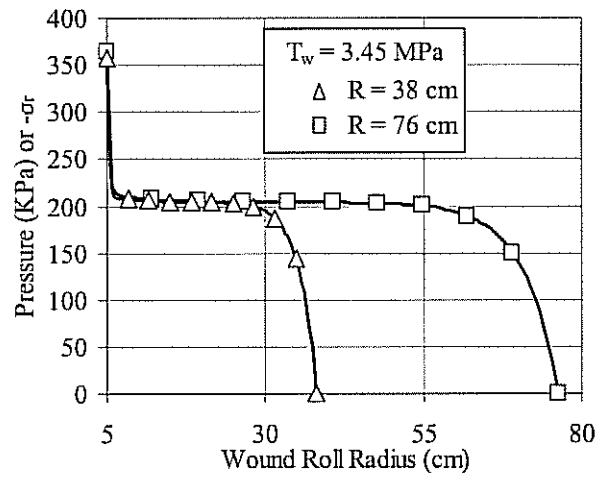

Figure 4 – Pressure ($-\sigma_r$) in a Roll Wound of Fine Coated Paper in the *Spongy* State

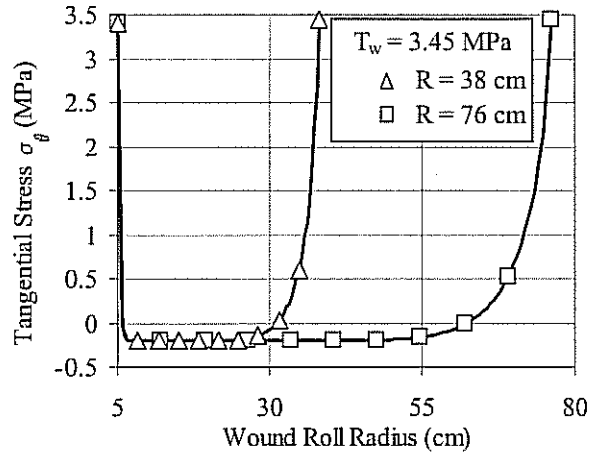

Figure 5 – Tangential Stress (σ_0) in a Roll Wound of Fine Coated Paper in the *Spongy* State

The *spongy* behavior was obtained by winding this paper at a constant winding tension of 3.45 MPa as shown by the pressure and circumferential stresses shown versus wound roll radius in Figures 4 and 5. Note that the results are given for two different final wound roll radii, 38 and 76 cm. This allows us to study how the selection of the finished radius affects the internal stresses within the wound roll. For rolls that exhibit *spongy* behavior it is shown that only the only effect of final radius is to extend the range of the radius in which the pressure and circumferential stress are constant. These analyses only consider the stresses due to winding and not those due to the dead weight of the wound roll which are not axisymmetric and are dependent whether the roll is supported by the core, at the perimeter, or upon the end.

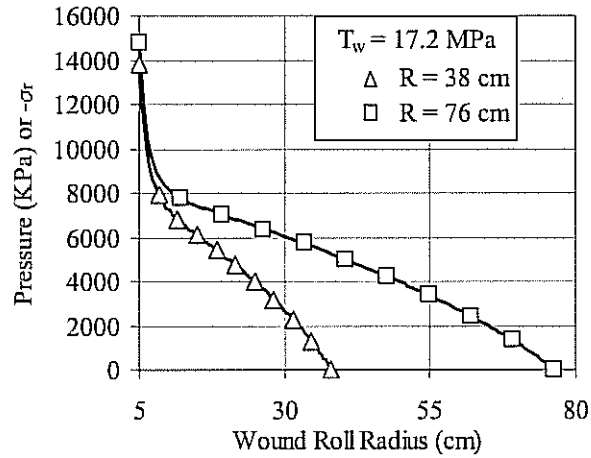

Figure 6 – Pressure ($-\sigma_r$) in a Roll Wound of Fine Coated Paper in the *Fully Compressed* State

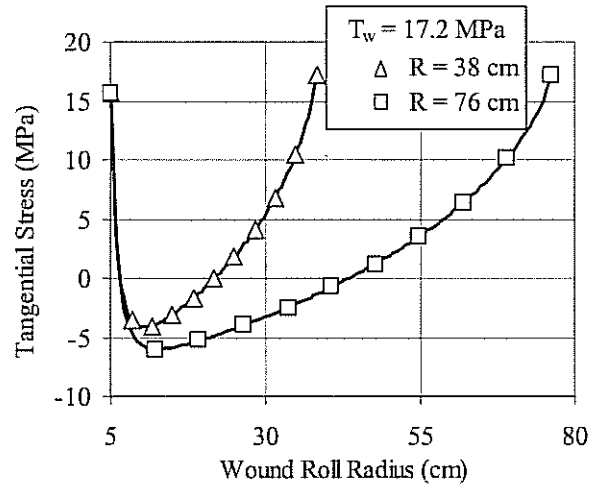

Figure 7 – Tangential Stress (σ_θ) in a Roll Wound of Fine Coated Paper in the *Fully Compressed* State

The *fully compressed* behavior is demonstrated by the same web when the winding tension is increased to 17.2 MPa as shown in Figures 6 and 7. Now it is evident that winding larger rolls causes the pressures to increase at all radii and alters the circumferential stresses at all radii except those near the core and the final radius. Note as well that the negative circumferential stresses have increased substantially due to increased winding tension and the shift from *spongy* to *fully compressed* behavior when comparing the results in Figures 5 and 7.

In cases in which the web is very compressible in the radial direction combined with moderate to high winding tensions all models which employ an outer boundary condition similar to expression {12} will produce internal pressures as a function of radius which are greater than those measured by experimental means. Expression {12} was derived using a thin wall pressure vessel equilibrium equation which incorporates an assumption that the internal pressure is an independent input variable. In the cases in point the outer surface of the winding roll is hardly rigid, and the interface beneath the outer layer and the layer beneath deform inward as the incoming web becomes the outer layer of the winding roll. Good et al [16] reformed the outer boundary condition as:

$$\delta\sigma_r\big|_{r=s} = -\left(T_w\big|_{r=s} + \frac{u\big|_{r=s}}{s} E_\theta \right) \frac{h}{s} \qquad \{18\}$$

where u is the radial deformation of the interface (always negative) which results in a tension loss term and a pressure beneath the outer layer which is less than that predicted by expression {12}. When this boundary condition was implemented in a winding model similar to Hakiel's, the model produced internal pressures which compared well with those measured in the laboratory.

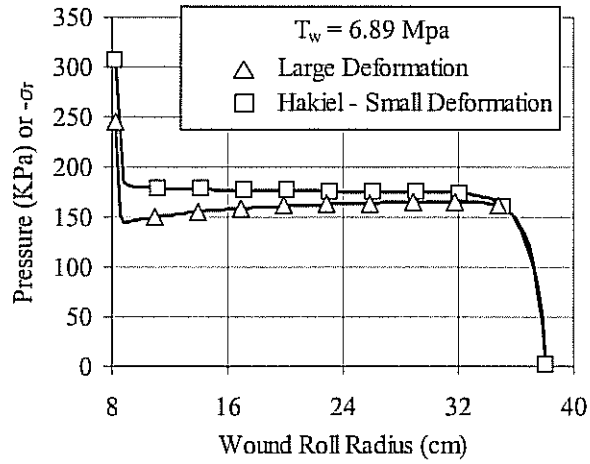

Figure 8 – Radial Pressures in Newsprint Rolls using Small and Large Deformation Models

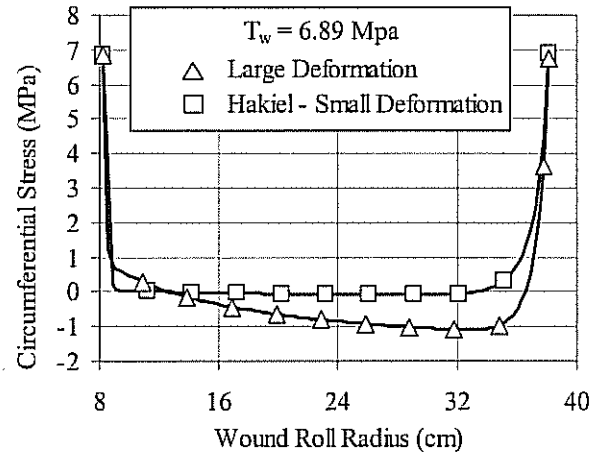

Figure 9 – Circumferential Stresses in Newsprint Rolls using Small and Large Deformation Models

For those webs which exhibit high radial moduli, the radial deformation of the interface (u) will be small and expression {12} will produce accurate results. Benson [9] later produced a model which accounted for large deformations within the roll which embodied a constraint similar to that of expression {18} and produced results which were comparable to those of Good et al [16]. These models must compute deformation to be able to implement the outer boundary condition of expression {18}. An example of the output of a model which incorporates this modified boundary condition is shown in Figures 8 and 9 for newsprint wound at a constant winding tension of 6.89 MPa. Note the large deformation models predict less pressure and significantly less circumferential stress in the wound roll.

Typically one dimensional plane stress winding models produce outputs which include the radial pressure and the circumferential stress as a function of radius. These models can be useful for anticipating a number of roll defects in narrow rolls in which the pressures and circumferential stress are uniform across the roll width. Defects are the subject of a later section, herein.

Plane Strain Winding Models. In plane stress all z dimension stresses are assumed to be zero which resulted in the constitutive relationships presented in expression {2}. Wound rolls are often quite wide compared to the diameter and one might assume that plane strain conditions prevail.

$$\varepsilon_r = \frac{\sigma_r}{E_r} - \frac{\nu_{r\theta}\sigma_\theta}{E_\theta} - \frac{\nu_{rz}\sigma_z}{E_z}$$

$$\varepsilon_\theta = -\frac{\nu_{\theta r}\sigma_r}{E_r} + \frac{\sigma_\theta}{E_\theta} - \frac{\nu_{\theta z}\sigma_z}{E_z} \qquad \{19\}$$

$$\varepsilon_z = 0 = -\frac{\nu_{zr}\sigma_r}{E_r} - \frac{\nu_{z\theta}\sigma_\theta}{E_\theta} + \frac{\sigma_z}{E_z}$$

ASTM[1] has set the following criteria to determine when plane strain conditions exist. When the width (W) of a fracture specimen exceeds the criterion set in the following expression:

$$W \geq 2.5\left[\frac{K_{IC}}{\sigma_{ys}}\right]^2 \qquad \{20\}$$

plane strain conditions will prevail. Materials with low plane strain fracture toughness compared to the yield strength may require very little specimen width to achieve plane strain conditions. For polyester the plane strain fracture toughness can range in the domain of 1.09 to 1.70 MPa$\sqrt{m}$ and the yield stress can range in the domain of 33 to 40 MPa. Per expression {20} plane strain conditions should prevail for wound rolls of polyester which are about 3.6 mm and wider.

Maxwell's relation was introduced earlier in the plane stress derivation in expression {7}. Now that the constitutive relations have been expanded in expression {19}, Maxwell's relations can be expanded as well:

$$\frac{\nu_{r\theta}}{E_\theta} = \frac{\nu_{\theta r}}{E_r} \quad \frac{\nu_{rz}}{E_z} = \frac{\nu_{zr}}{E_r} \quad \frac{\nu_{\theta z}}{E_z} = \frac{\nu_{z\theta}}{E_\theta} \qquad \{21\}$$

If the constitutive expressions {19}, the equilibrium expression {1}, the compatibility expression {9} and Maxwell's expressions {21} are combined, the following second order differential equation in radial stress results:

$$r^2\frac{d^2\delta\sigma_r}{dr^2} + 3r\frac{d\delta\sigma_r}{dr} + \left(\frac{E_\theta^2\left(E_z\nu_{zr}^2 - E_r\right)}{E_r^2\left(E_\theta - E_z\nu_{z\theta}^2\right)} + 1\right)\delta\sigma_r = 0 \qquad \{22\}$$

The similarity between expressions {22} and {11} should be noted. Also if ν_{zr} and $\nu_{z\theta}$ approach zero, it should be noted that expression {22} becomes expression {11}. As mentioned earlier it is common that the Poisson's ratios with an r component are on the order of 0.01 and smaller. Thus the largest difference between expressions {22} and {11} lies within the E_θ-$E_z\nu_{z\theta}^2$ terms in the denominator of the third term. For a web with equivalent MD and CMD modulus (E_θ=E_z) and with a $\nu_{z\theta}$ of 0.3 this term would become about 91% of E_θ and thus may not have a large impact on the resulting internal stresses. The strain in the first layer is:

[1] American Society for Testing and Materials, ASTM STP 410, 1966.

$$\varepsilon_\theta = \frac{u}{r_c} = u\Big|_{r=layer1} = \frac{\delta\sigma_\theta}{E_\theta} - \frac{\nu_{\theta r}\delta\sigma_r}{E_r} - \frac{\nu_{\theta z}\delta\sigma_z}{E_z} = \frac{1}{E_\theta}\left(\delta\sigma_\theta - \nu_{r\theta}\delta\sigma_r - \nu_{z\theta}\delta\sigma_z\right)\Big|_{r=layer1} \quad \{23\}$$

This expression is equated with expression {13}. Using the equilibrium expression {1} and the constitutive expressions {19} the derivative boundary condition at the core can be cast in form:

$$\frac{d\delta\sigma_r}{dr}\Big|_{r=1} = \frac{E_\theta^2 + E_c\left(E_z\nu_{z\theta}^2 + E_\theta\left(\nu_{r\theta} - 1 + \nu_{rz}\nu_{z\theta}\right)\right)}{E_c\left(E_\theta - E_z\nu_{z\theta}^2\right)}\frac{\delta\sigma_r}{r_c}\Big|_{r=1} \quad \{24\}$$

If ν_{rz} and $\nu_{z\theta}$ are allowed to approach zero note that expression {24} becomes expression {15}. Again if the Poisson's ratios with r component are the common small values the largest difference between expressions {24} and {15} fall within the E_θ-$E_z\nu_{z\theta}^2$ terms. In Figures 4 and 5 the pressure and circumferential stresses were presented for winding fine coated paper at a constant winding tension of 3.45 MPa based upon a plane stress winding model.

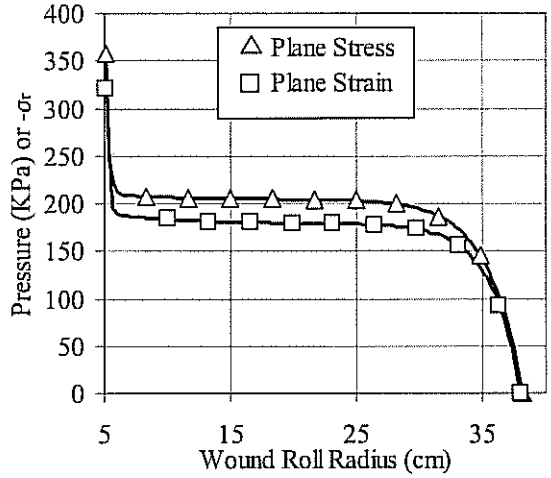

Figure 10 – Pressure Comparison for Plane Stress vs. Plane Strain Conditions for FCP

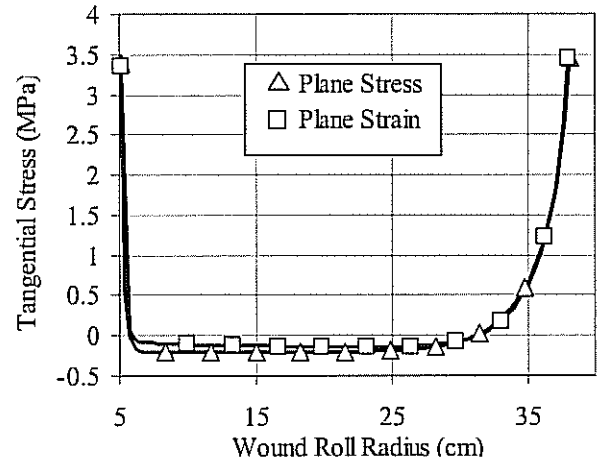

Figure 11 – Circumferential Stress Comparison for Plane Stress vs. Plane Strain Conditions for FCP

Now in Figures 10 and 11 the same winding case is presented again comparing the plane stress and plane strain model formulations. The plane strain formulation shows about an 12% reduction in pressure. The circumferential stresses are hardly distinguishable from one another in Figure 11. The axial stresses for the plane strain formulation are shown in Figure 12.

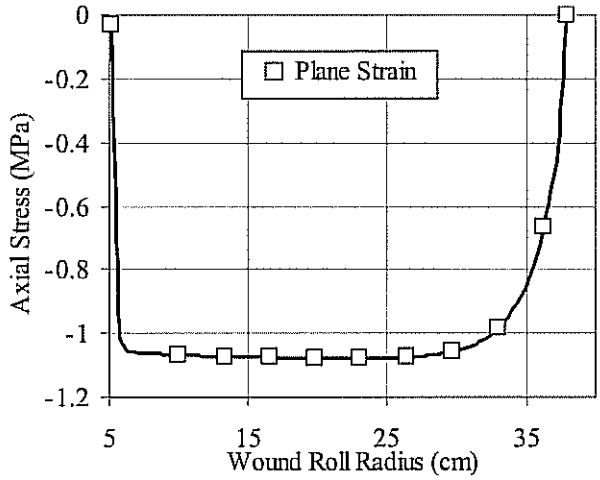

Figure 12 – Axial Stress for Plane Stress vs. Plane Strain Conditions for FCP.

Typically one dimensional plane strain winding models produce outputs which include the radial pressure, the circumferential stress, and the axial stress as a function of radius. Expressions such as expression {20} should be used to determine whether plane stress or plane strain conditions prevail. Again these models can be useful for anticipating a number of roll defects in narrow rolls in which the pressures, the circumferential stress and the axial stress are uniform across the roll width.

Two Dimensional Center Winding Models

A few two-dimensional models exist that allow one to predict how the internal stresses vary with respect to radius and cross machine direction (CMD) location. The need for such models arose due to the inability to produce webs with constant thickness. The variation in thickness may be due to non-uniformity in the forming or drying process in making paper, the extrusion processes by which plastic films are produced, and the rolling processes by which metal foils and strip are made. Thickness non-uniformity is pervasive throughout web industries due in some part to the processes by which the web is made and due also to the methods by which the webs are coated. Webs are sometimes buildups of multiple webs, some of which may not be continuous across the width. Thus the thickness of some webs is non-uniform by design. Thickness non-uniformity is most destructive within wound rolls when the non-uniformity occurs in the cross machine direction but is in fact uniform in the machine direction. The result of additional web thickness locally compiles as the roll winds. Wound rolls often consist of thousands of web layers, thus a web which is locally a few percent thicker in one CMD location is apt to have a large local anomaly in the outer radius of the wound roll at that CMD location. Those who categorize defects call these anomalies circumferential ridges or hard streaks [17]. These ridges may produce bursts during winding given sufficient amplitude or may

produce length non-uniformity across the width through time due to viscoelastic response within the wound roll.

The first two dimensional models were extensions of one dimensional models. The web thickness would be profiled in the CMD and the web width would be parsed into segments. Each segment would be assigned a nominal thickness and would be modeled using a one dimensional model such as Hakiel's one dimensional model which was described earlier. These models were limited to center winding but the allocation of web tension across the web width is a key point in these models. The sum of all of the tensions in each segment across the width should be equivalent to the total web tension in the winder tension zone.

Kedl [18] assessed how the winding tension varied across the roll width by modeling the deformation of the outer layer of the winding roll as a beam resting upon an elastic foundation (which was comprised of the segments of stacks of web beneath the outer layer). He then assumed that the angular velocities of all the segments were common. From continuity Shelton [19] derived that in steady state that a web, at strain ε_o and velocity V_o at one location, which increases to a velocity V_i downstream will assume a higher strain level ε_i at that downstream location. The wound roll may vary in radius (r_i) as a function of cross machine direction location, as shown in Figure 13, but the angular velocity ω of the wound roll is constant thus Shelton's equation becomes:

$$(1-\varepsilon_o)V_o = (1-\varepsilon_i)V_i = (1-\varepsilon_i)r_i\omega \qquad \{25\}$$

The angular velocity of the wound roll is calculated by dividing the upstream web velocity, assumed constant across the web width, by the average wound roll radius. The web tension is then parsed to each CMD segment using the expression:

$$T_{wi} = E_\theta\left[1-\frac{V_o(1-\varepsilon_o)}{r_i\omega}\right] \qquad \{26\}$$

where ε_o is the MD strain due to uniform web tension at the upstream end of the winder tension zone. Those segments with outer radii greater than the average radius receive a greater allocation of web tension than those segments whose outer radius are equal to or less than the average radius. Kedl then employed a one dimensional winding model developed by Struik [15] to determine the internal pressure and circumferential stresses in each sector subject to the winding tension developed in expression {26} for that sector. Kedl verified his model using force sensitive resistors to infer the roll pressures at several locations in the cross machine direction and at several radial locations.

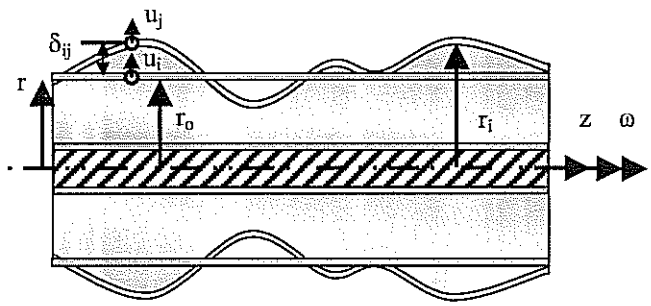

Figure 13 – Definition of Relaxation Radius in Two-Dimensional Winding

Hakiel [20] developed an algorithm to parse the web tension by a different method. He developed the concept of a relaxation radius R_o for a new outer lap of web to be added

to the outside of the wound roll. Hakiel then enforced radial displacements due to interference between the outside of the previous layer and the new layer being added. This induced higher web tension at the high radius locations in the wound roll and lower tensions at the smaller radius locations. After determining the tension variation across the width for an assumed relaxation radius, the tension (in units of stress) would be integrated across the width and thickness of the outer layer and compared to the web tension. If the integrated tension was larger than the web tension the relaxation radius would be increased and the process repeated until the integrated tension and the applied web tension matched. Hakiel's expression for the parsed web tension was:

$$T_{wi} = \frac{E_\theta}{1-\nu^2}\left[\frac{r(i,j)-r_o(i)}{r_o(i)}\right] \qquad \{27\}$$

Gapping (the separation of layers) was possible in this algorithm by not allowing r(i,j) to be less than the relaxation radius $R_n(i)$. The parsed tensions across the width were then applied locally to one-dimensional winding models such as Hakiel's [7] which was previously discussed, the incremental stresses were calculated and used to update the total stress in each widthwise segment, the outside radius was updated, and finally the process was repeated for a new outer lap. Later Cole and Hakiel [21] presented an improved model which coupled computed in-roll displacements to a modified version of expression {27}. Cole verified his model by inferring core pressure through measured strains on the surface of a segmented core and by documenting the shape of the outside of the winding roll using a profilometer.

The next advance was the development of true two-dimensional wound roll models that no longer treated the wound roll as a series of sectors each of which could be modeled independently with an existing one dimensional winding model. The models of Hakiel, Cole and Kedl ignored the compatibility of deformation of a given layer as it passed from one sector to the next. These models relied upon the solution of a second order differential equation in incremental pressure, similar to expression {11}. Thus the internal deformations within the consecutive sectors of a given layer were never compared and displacement compatibility at the interfaces between sectors was not enforced. The model developed by Hoffecker and Good [22] employs an axisymmetric finite element method. A series of quadrilateral elements were used to model a layer or group of layers in the wound roll. The web thickness is allowed to vary lineally across the width of each quadrilateral. The primary output of finite element codes in solid mechanics are nodal deformations. Strains and stresses are secondary outputs as they depend on knowledge of the deformation of the finite elements. A facet of all winding models is the requirement of an accretive solution. Thus as each layer is accreted onto the outside of the winding roll the new outside radius of the winding roll is part of the primary solution vector. The core boundary condition discussed earlier for one dimensional models is automatically satisfied by the two dimensional models. The core is an integral component of the axisymmetric finite element model. The first few layers of quadrilateral elements model the core. The one dimensional models incorporate a core stiffness E_c in one dimension per expressions {13-15}. The axisymmetric models allow any core which can be defined in the axisymmetric plane. Thus cores which are cylindrical tubes, cylindrical tubes with one or two end closures, cylindrical tubes supported by an expanding core shaft, or cylindrical tubes supported by an expanding core stub shafts can be modeled. Cylindrical cores with orthotropic properties in cylindrical coordinates could be modeled and those properties could potentially vary with core radius. Establishing the winding tension across the web width was accomplished using an interference method which employs the Lagrangian constraint method. Similar

to earlier models it was assumed that layers of web in the form of cylinders would be accreted to the outside of the winding roll. This cylinder would have a relaxed radius R_o prior to becoming the outer layer on the winding roll. This relaxation radius could vary, thus the cylinder becomes a generic axisymmetric shape, across the web width to accommodate length nonuniformity across the web width as well as the web thickness. The relaxation radius must be initially assumed which determines the level of interference δ_{ij} between the cylinder and the outside of the previous layer which was last added to the wound roll, refer to Figure 13. A Lagrangian constraint of the form:

$$u_j - u_i = \delta_{ij} \qquad \{28\}$$

is then enforced at several nodal points across the width of the winding roll. This is a relative constraint which forces the outer layer cylinder outward and the outside of the layer beneath inward until the two surfaces collocate to some radial position. The circumferential stresses σ_θ are then computed and averaged across the web width. This result will be equal to the average web line tension T_w, in units of stress, if the relaxation radius R_o was chosen correctly at the start. If the average computed circumferential stress is larger than the web line tension, then the assumed value of the relaxation radius was too small and the process must be repeated with a larger relaxation radius. This is an iterative process which ceases after the average circumferential stress and the average web line tension become equal. This process is not difficult computationally since several thousand layers typically comprise a wound roll and the relaxation radius used for adding the last lap is a good starting point assumption for the relaxation radius of the next lap to be added. Lee and Wickert [23,24] have formed models based upon axisymmetric finite element formulations as well. The principal difference in these works with respect to the work of Hoffecker and Good is the treatment of the tension in the outer layer. Whilst Hoffecker and Good assume that the current outer profile of radius across the width of the wound roll must affect the allocation of web tension across the width through the method discussed above, Lee and Wickert assume the widthwise distribution in tension is known prior to winding and that the shape of the wound roll does not impact this distribution. Including the effect of the widthwise radial profile on winding tension allocation was shown to be important in the works of Kedl, Hakiel, Cole and Spitz[25].

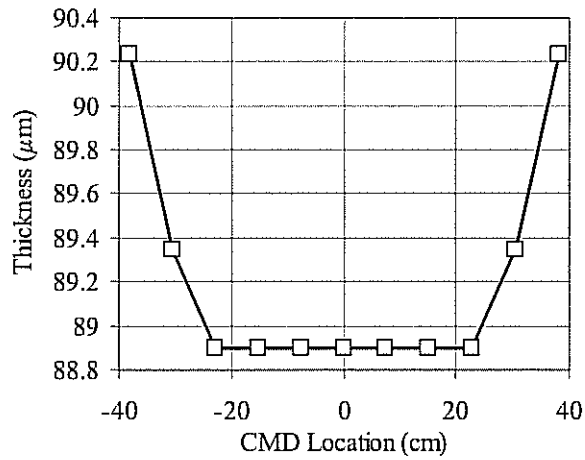

Figure 14 – Thickness Variation of Fine Coated Paper (FCP) vs. CMD

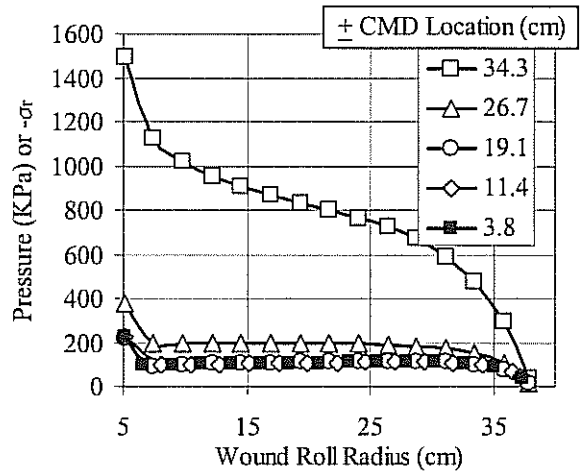

Figure 15 – Pressure in Rolls of FCP with the Thickness Variation shown in Figure 12.

To generate an appreciation for the importance of the effect of thickness variation over the width, consider the fine paper grade which was used in the earlier examples for one-dimensional winding models. In this example it will be assumed that the paper is 76.2 cm wide and has 1.5% greater thickness at the edges as shown in Figure 14. The web tension upstream of the winder will be assumed to be 3.45 MPa and the roll will be wound to a final radius of 38 cm on the aluminum core of the same dimensions used to produce the results in Figures 4 and 5 from the one-dimensional model. The results from the two-dimensional model of the type developed by Hoffecker and Good are shown in Figures 15 and 16.

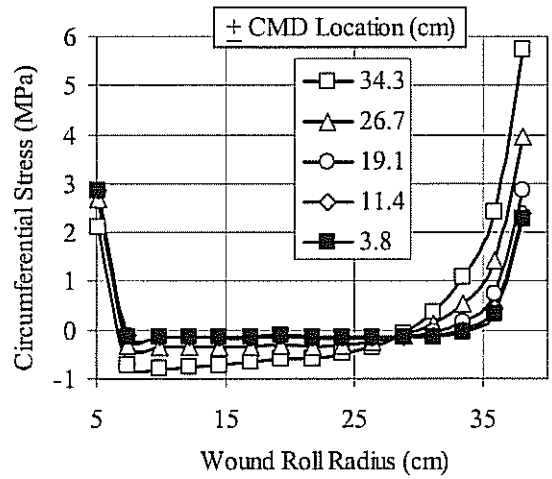

Figure 16 – Circumferential Stress in Rolls of FCP with Thickness per Figure 12.

Note the radial pressure at the edges of the web in Figure 15 is now approaching the *fully compressed* condition with pressures 4 to 5 times greater than those predicted for the web with uniform thickness in Figure 4. Also note in Figure 16 that the web circumferential stress in the web edges at the completion of the roll was nearly twice as large as the uniform web stress of 3.45 MPa, assumed to exist upstream. Since bursts increase

nonlinearly with web stress level it appears that a 1.5% increase in web thickness could dramatically influence productivity in this example. Also note that the negative circumferential stresses in the web edges in Figure 16, at 10 to 20 cm of wound roll radius, are over 600 MPa more negative than those shown for the uniform thickness web in Figure 5. This may be influential in the formation of edge buckles.

The outputs of two dimensional models include radial pressure, circumferential stress, axial stress and shear stress as a function of the axisymmetric location. Roll deformations are also available. Defects which can be predicted with two dimensional models will be treated in a later section.

APPLICABILITY OF WINDING MODELS TO VARIOUS WINDERS

All of the winding models discussed above assume that the tension in the outer layer of the winding roll is known. In fact this is known outright for a center winder, with no rider or nip roller. Such winders comprise only a small portion of the winders used in industry. Thus before defects can be predicted by winding models one must determine how to apply a winding model to whatever type of winder that is being used. To give the reader an appreciation of the diversity of winding equipment the section below attempts to describe various kinds of winding equipment. This will be followed by a section which focuses on how winding models can be used to determine what the internal stresses are in rolls wound on various types of winders.

Types of Winders

The winding methods which are used in the industry today can be broadly categorized into the following groups and are shown in Figure 17:

- Center Winder – The center winder is classified as such as the torque to wind the roll is provided to the center or core of the winding roll. The torque provided to the core is not necessarily constant and is often tapered to produce optimal internal residual stresses in the wound roll.
- Center Winder with Rider Roller – This winder is similar to the center winder except an idler roller, sometimes called a rider or nip roller, is pressed into contact with the outer surface of the winding roll. In some cases the idler roller may be tendency driven to ensure the roller is moving at web velocity. The web may contact the wound roll first or wrap the nip roller first. The torque required to wind the roll is provided through the core.
- Surface Winder – Physically this winder can appear similar to the center winder with a rider roller. The difference is that the torque to wind the roll is now provided through the rider or nip roller and the core is not driven. The nip roller is typically driven at a programmed velocity. Surface winders are prevalent in situations where web thickness may vary significantly across the web width where center winding would result in a winding roll with non-uniform radius that could eventually result in a burst or quality loss due to corrugations and fold overs.
- Differential Torque Winders – A differential torque winder mechanically appears similar to a center winder with a rider roll or a surface winder. The only difference is that now substantial torque is provided to both the core and the rider roller. Typically the rider or nip roller is driven in velocity control and the core is driven in torque control. Both the rider and the core may be driven in torque control but it is more common to provide velocity control to the rider to

prevent runaways. Sometimes this type of winding is called surface winding with center torque assist. The assist torque to the core may not be large, in fact it is often just sufficient to overcome bearing drag on the center shaft, the rolling resistance between the rider and the winding roll, and other loss factors. This type of winder is often the only solution when winding webs whose surfaces have low coefficient of friction. This type of winder is common in slitting operations. The incoming web is slit on the roller in velocity control and then independent torque can be provided to the cores of each slit.

- Two Drum Winders – These winders are popular in the paper and textile industries and are known for their high productivity. In this winder the web wraps a first drum (a drum is a large diameter roller) which is in velocity control, wraps about the winding roll, proceeds beneath a rider roller which is impinged into the winding roll, wraps the winding roll further and passes beneath a second drum which is in torque control, and finally proceeds and passes beneath the first drum again where the outer layer of web becomes the second layer in the winding roll. This method of control describes a majority of two drum winders but there are certainly cases in which the second drum is controlled in a draw mode (differential velocity) with respect to the first drum and other cases where both drums could be running in torque control. The productivity of this winder can be quite high as the core is handled minimally. Two drum winders are often used as rewinders following the paper making process. One of the difficulties of two drum winders is the uncontrollable nip load due to the dead weight of the winding roll resting upon the drums which could lead to high web tensions that could burst the web. This effectively limited the weight and thus the diameter of the rolls which could be wound on this type of winder. Some recent designs focus on decreasing the nip load between the drums and wound roll by pressurizing the air between the two drums, resulting in lift on the wound roll. Other designs have moved to compliant drum coverings in an effort to decrease the web tension in the winder.
- Belted Winders – Some webs such as tissues and others cannot be subjected to rider rolls and high nip loads without the loss of loft. Fragile webs such as these are sometimes wound on belted winders. The benefit of this type winder is minimal nip load and thus minimal compaction of a high loft web. The majority of the energy required to wind the roll is provided to the rollers upon which the belt is driven. In some cases some center assist torque may be input to the core.

There are other types of winders which exist which do not fall precisely into the categories listed, but the groups presented here comprise a large majority of the winders used commercially. In other cases one may find subgroups of winders that fit amongst one of the larger groups mentioned here. Gap winders are an example. Physically gap winders appear very much as a center winder with a rider roller. Upon close observation it is found the rider roller is not impinged into the winding roll, in fact there is an air gap between the rider and wound roll. Thus a gap winder is a center winder and can be very useful when wrinkling is a problem on the wound roll. The web wraps the idler prior to contacting the wound roll and the short span prevents wrinkles and fold-overs from occurring which can be useful on webs with thickness variation. A second example would be a winder in which the configuration is largely that of the two drum winder where the second drum is replaced with a belt support. The winding torque which ordinarily would have been supplied by the second drum would now be applied via the

belt drive. The benefit of the belt support is a reduction in nip-induced slippage and hence a decrease in the maximum tension in the web which allows rolls of greater diameter to be wound prior to web burst failures.

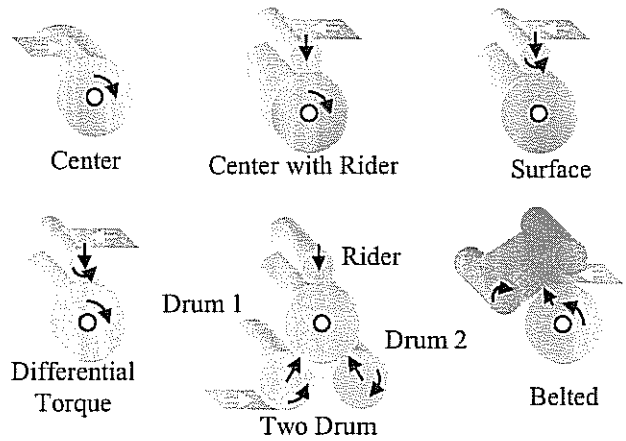

Figure 17 – Basic Winder Types. (White arrows depict direction of web travel, black arrows depict nip loads, and curved arrows depict potential torque inputs)

Wound-On-Tension (WOT)

Rolls which are center wound without a rider roll represent a minority of the winding done in production facilities today. Almost all of the one dimensional center winding models discussed in the section on wound roll models include an assumption that the web line tension (T_w) becomes the circumferential stress in the outer layer of the winding roll. The one exception was the case in which the radial deformations during winding at the outer layer were so large that tension in the outer layer became less than the web tension [16]. The majority of rolls are wound with some sort of a roller impinged into their outer surface using one of the winding methods described in the previous section. These impinged rollers may increase or decrease the tension in the outer layer, the Wound-On-Tension (WOT), to a level above or below the web tension just prior to the winder.

WOT on Center Winders with Rider or Nip Rollers and Surface Winders. The primary difference between a center winder and all other winders is the influence of an impinged roller, often called a nip roller. Pfeiffer [26] acknowledged this as a result of performing Cameron Gap tests on rolls that had been wound on a two drum winder. He coined a new term "Wound-In-Tension," which was the tension in the current outer layer of a winding roll, and discussed how this tension was higher than the web tension just upstream of the winder for a roll wound with impinged nip or rider rollers. The nip roller induces slippage between the outer layers of a winding roll. The first insight in the literature that this slippage was occurring came also from Pfeiffer [27]. Pfeiffer conducted experiments in which he rolled nip rollers of various radii and weights over stacks of web which were restrained by force transducers. What he found was that the uppermost layer always slipped in the direction of the rolling nip above the sheets beneath inducing an additional tension in the outermost layer. He also used the "instant center of rotation" concept, a concept often used in studies of dynamic systems. The instant center is the point that all motion appears to be rotating about at an instant in time.

In the case of a rigid cylinder rolling over a rigid half plane the instant center is located at the line of contact between the cylinder and the plane. Pfeiffer proved with micrographs that when rolling a cylinder over a stack that this instant center was located vertically 2 to 3 web layers beneath the cylinder. Thus those 2 to 3 layers moved in the rolling direction of the cylinder (adding tension to those layers) whilst those beneath the instant center could move in the opposite direction.

Rand and Eriksson [28] documented the slippage and tension increase due to impinged nips by applying strain gages to a newsprint web and recording the machine direction strain as the instrumented web was wound into rolls. These tests were conducted on center winders, center winders with nips, and two drum winders. This work was key in that it documented the increases in tension in the outer layer as it passed under the nip roller(s) in the winders. It was also evident in these tests that the circumferential tension in a given layer was maximum as it was wound onto the roll and then decreased as successive layers were then wound outside of it. This phenomenon is also evident from the results of the winding model, refer to Figures 5 and 7. In center winding tests with a rider or nip roll, the passage of the nip roll was seen as a transient in the data in the second layer and those layers beneath although there was a step change in tension in the outer layer as it passed beneath the nip roller, refer to Figure 18. This step change is called the nip-induced-tension (NIT). This leads to a conclusion that the permanent effect of the nip roll on wound roll internal pressures and stresses occurs primarily due to the slippage induced beneath the outer layer. The pressure which is increasing beneath the successive layers below the outer layer acts to inhibit slippage beneath those layers.

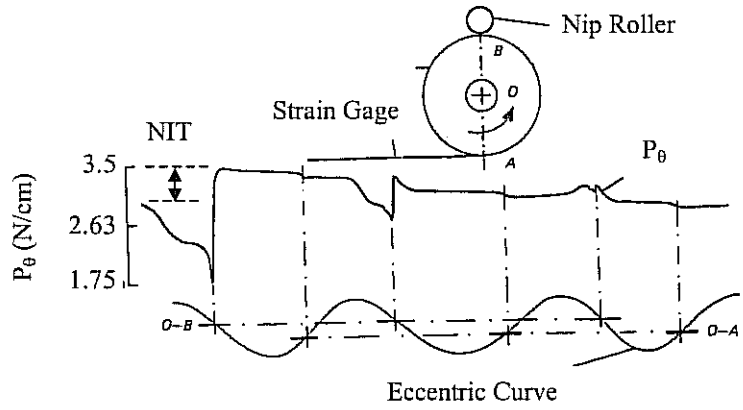

Figure 18 – Circumferential Loads in a Paper Web Wound into a Center Winder with an Undriven Nip Load. *(Reprinted with the permission of L.G. Eriksson)*

Further evidence of the impact of a nip roller impinged into the winding roll was provided by Pfeiffer [29]. Pfeiffer developed a means of measuring the wound-in tension in the outer layer on a surface winder. After the outer layer passed beneath the incoming nip roll it was pulled away from the surface of the winding roll, wrapped about an idler mounted upon force transducers, and was finally allowed to return to the surface of the winding roll. This was the first convenient means of directly studying the tension in the outer layer of a roll wound in the presence of a nip as a function of winder operating parameters including incoming web tension and nip load that could be varied during the

test. Pfeiffer found that increased nip load and incoming web tension caused the wound-in tension to increase, again direct evidence that the nip roller was key in regulating the amount of slip between the outer layer and the layer beneath. Although Pfeiffer's apparatus was setup in a way in which web tension and nip load were not completely independent his findings were still very important. Pfeiffer also developed a wound-off tension measurement that allowed study of the tension in the outer layer during unwinding [30]. Theoretically, if there were no hysteretic or viscoelastic losses, the wound-in and wound-off tension records would be identical. Pfeiffer produced a wound-off tension plot for the same roll that he produced a wound-in tension plot in the earlier publication. The two plots were similar qualitatively but there were magnitude differences that were due to the loss terms and interdependence between wound-in tension and nip load during winding. The concept of the wound-off-tension method was novel in that it provided a technique by which a roll could be wound on any winder under any winder operating parameters but through unwinding the wound-in-tension could be deduced. When the wound-in-tension was coupled with a wound roll model the internal pressures and stresses of winding could be known.

Good and Fikes [31] studied the pressures in rolls which were center wound with a rider roller (an undriven or idling nip roller). In this study force sensitive resistors were used to document the pressures in the wound roll after winding was complete. Using a wound roll model in the style of Hakiel [7], the tension in the outer layer in the winding roll was iterated until the model produced pressures of like magnitude to the experimental results. At this point the wound-in tension coined by Pfeiffer was re-coined as the Wound-On-Tension or WOT. The chief finding in this study was that the WOT was directly affected by web tension prior to the winder and affected through a constant of proportionality to the nip load. The constant appeared to be similar in magnitude to the kinetic coefficient of friction and thus the first WOT algorithm for center winding with an undriven nip roller was generated:

$$WOT_{CenterWinding\_with\_nip} = T_w + \mu_k \frac{N}{h} \qquad \{29\}$$

where the web tension (T_w) has units of stress, the nip load (N) has units of load per unit width of nip contact, and the web thickness (h) has units of length, thus the WOT has units of stress.

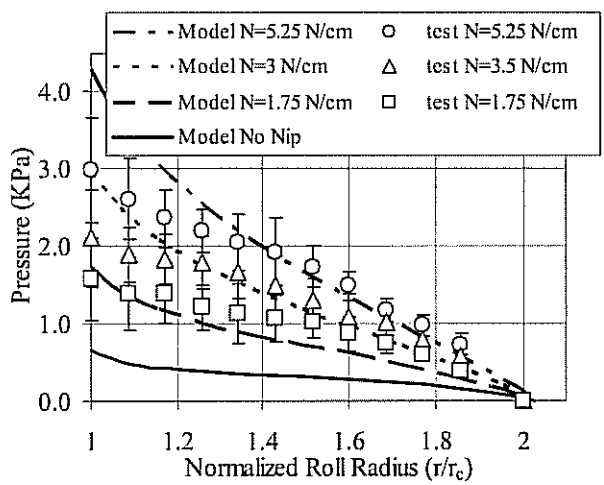

Figure 19 – Pressures within Wound Rolls of Polypropylene Wound without a Nip and with a Nip at Various Load Levels.

This WOT could replace the web tension in the outer wound roll boundary condition of expression {10} or:

$$\delta\sigma_r\big|_{r=s} = -\frac{WOT\big|_{r=s}}{s}h \qquad \{30\}$$

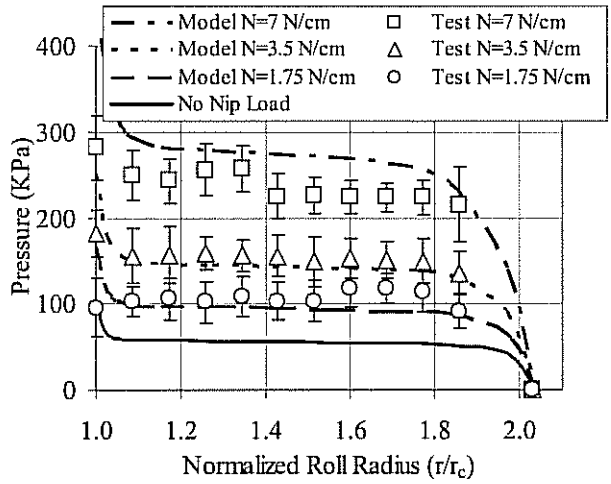

Figure 20 – Pressures within Wound Rolls of Light Weight Coated Paper without a Nip and with a Nip at Various Load Levels.

This new boundary condition could then be used with a wound roll model to produce the internal pressures and circumferential pressures within the wound roll when winding with a center winder with an impinged undriven nip roller. The boundary condition was proven to work well for winding rolls of polypropylene film and rolls of light weight coated paper, refer to Figures 19 and 20, respectively. In another reference it was shown that this worked well for bond paper as well, results from which are shown in Figure 21 [16].

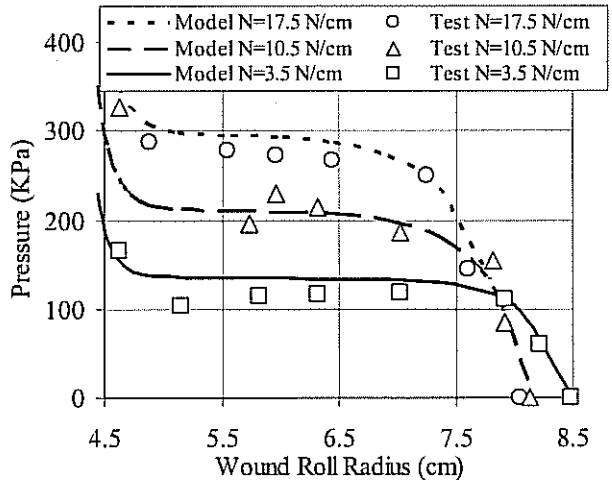

Figure 21 – Pressures within Wound Rolls of Bond Paper with a Nip at Various Load Levels.

At this point a dichotomy in the literature existed. Pfeiffer's work [27] of rolling nips over stacks suggested that slippage was occurring throughout several layers and in fact the direction of slippage reversed with layers at greater depths in the stack. The results of Rand and Eriksson's study [28] suggested most of the slippage was occurring in the outer layer which was supported by the work of Good and Fikes [31] where they proved that by altering only the WOT in the outer layer that roll pressures produced by wound roll models were very similar those measured in the laboratory. Good, Wu, and Fikes [32,33] began a study to determine the mechanism of the slippage through a combination of finite element modeling computations, rolling nip mechanics tests over stacks similar to Pfeiffer's work [27], and winding tests in the laboratory. The findings of greatest importance in this work were that:

1. The increase in tension in the outer layer was due to micro-slip in the Hertzian contact zone beneath the nip between the outer layer and the layer beneath. The results of the finite element analysis indicated that the level of the increase in web tension was dictated by the peak magnitude of the tensile strain prior to any sticking behavior between the two layers. At low nip loads, where there was no stick behavior, the maximum tensile strain occurred at the center of the nip contact zone. Hertz's theory was developed for spheres and cylinders in contact with infinite half planes and in that case the strains due to contact are compressive in all dimensions. Johnson [34] and others have shown that extensional strains which would induce tensile stresses develop when rolling over layers of finite thickness.
2. The rolling nip mechanics studies over stacks were similar but not identical to Pfeiffer's. Dead weights were placed upon the stack before and after the rolling nip to simulate the interlayer pressure due to winding. Under these tests conditions the tension increased only in the uppermost or outer layer of web. All the layers beneath the outer layer showed no increases or decreases. The tension in the upper layer increased linearly initially with nip rolling distance until it saturated at an increased level which was $\mu_k N$ higher than the pretension which represented the web tension (T_w). This provided an alternate justification of use of expressions {29,30}.
3. With all or the majority of the slippage induced by the nip occurring beneath the outer layer it was concluded that winders with impinged nip rollers could be modeled using existing center winding models provided the WOT was known for that type of winder.

Pfeiffer's WOT apparatus [29] was a surface winder. His results indicated the WOT in surface winding was proportional to nip load and independent of web tension at low nip loads. At higher nip loads the dependency on nip load appeared to decrease but the WOT became dependent on web tension. At the highest nip loads tested, an increase in web tension resulted in nearly the same increase in WOT. Steves [35] surface wound rolls of news print. He inserted pull tabs while winding the rolls such that he could document the internal pressure as a function of wound roll radius. A pull tab is a piece of steel shim stock within an envelope of brass shim, the dissimilar metals exhibit a low friction coefficient. After winding a force gage was used to determine the force required to dislodge the steel shim and with knowledge of the friction coefficient the pressure can be inferred. A winding model of the form of Hakiel [7] was then employed by iterating the WOT until pressures like those found from tests were produced. Steve's then compared his WOT data to that of Pfeiffer and found good qualitative agreement at all nip loads but his results did not agree quantitatively with those of Pfeiffer, see Figure 22.

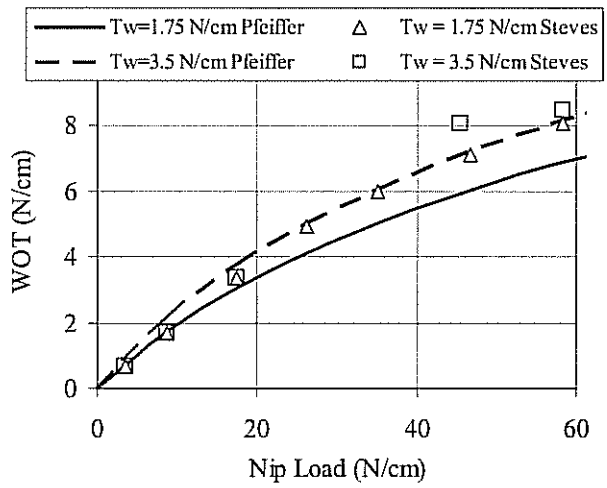

Figure 22 – A Comparison of WOT Data for Surface Winding Newsprint – Pfeiffer [29] vs. Steves [35]

The potential for quantitative discrepancy was highly probable since the properties of the news print used in the two investigations were undoubtedly different and the methods for ascertaining the WOT were quite different. A result from Steve's work was a WOT algorithm for surface winding which was known to be valid for nip loads up to 17.5 N/cm for news print. The WOT algorithm was:

$$WOT_{SurfaceWinding} = \mu_k \frac{N}{h} \quad N \le 17.5 \frac{N}{cm} \text{ news print} \qquad \{31\}$$

Later a study by Good, Hartwig, and Markum [36] set out to ascertain how the WOT differed between a center winder with an impinged nip roller and a surface winder. A secondary objective was to develop a comparison of the methods for determining the WOT which had previously been used by Pfeiffer [29] and Steves [35]. A new WOT apparatus was developed where nip load and web tension were truly independent winder operator input parameters. This was accomplished by wrapping the nip roller with the web by π radians and by maintaining the links which supported the nip roller in a vertical attitude by supporting them on a sled upon linear ways as shown in Figure 23.

The vertical attitude was maintained through a closed loop control system that measured the attitude of the linkage and then provided a proportionate command signal to a drive system which positioned the sled. The findings of this work included:

1. The direct measurement of WOT by extracting the outer layer after passing under the nip is an interfering experimental method. Trials using the pull tab method and a wound roll model to assess WOT did not agree with direct measurements when winding rolls of identical webs under identical winder operating conditions, refer to Figure 24.
2. The problem with the direct WOT measurement was the potential for slippage of the web between the point it passed beneath the nip and the point it was extracted from the surface of the wound roll (the arc angle having a magnitude ϕ) to make the WOT measurement. It was proven that when this slippage was occurring the directly measured WOT divided by the capstan slippage coefficient ($e^{\mu k \phi}$) was equivalent to the WOT inferred from pull tabs and use of

the wound roll model where the web was never extracted from the surface of the wound roll, again refer to Figure 24.

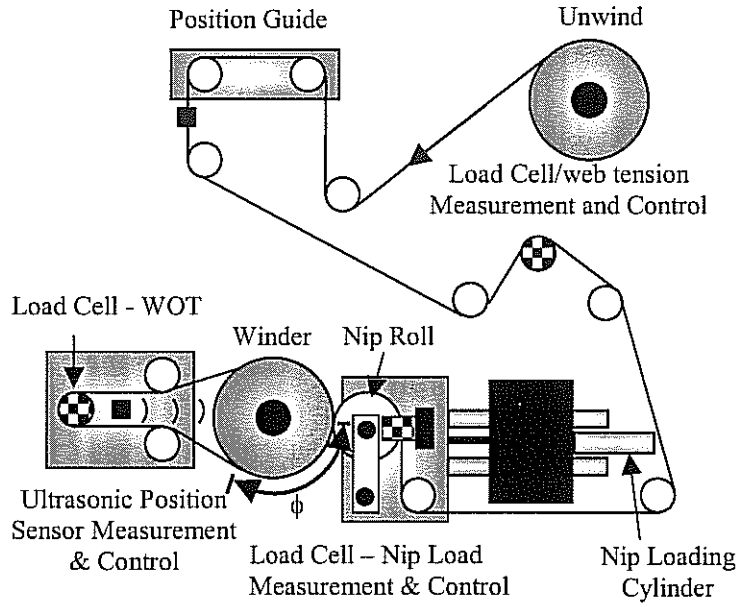

Figure 23 – Schematic of Good et al [36] WOT apparatus

3. That indeed at low nip loads the WOT for center winding with an undriven nip roller was given by expression {29} and the WOT for surface winding was given by expression {31}.
4. At higher nip loads it was apparent that there was a saturation level for the WOT in center winding and WOT became less dependent on nip load. A similar behavior was noted for surface winding but a dependence of the WOT on web tension developed with increased nip load, see Figure 24. This behavior was noted in Pfeiffer's work also [29].

At this point the behavior had been well measured for a very few webs but the range of applicability of expressions {29} and {31} was unknown for a generic web unless the WOT experiments were performed on that web. Thus from the modeling perspective expressions {29} and {31} might have been accurate for a generic web but at some unknown nip load the actual WOT would become less than that predicted by the expressions.

It was recognized at this point that contact mechanics computations would be required to provide additional accuracy in estimating the WOT. This was unfortunate in that this type of computations preclude the existence of closed form formulas of the simplicity of {29} and {31} over the entire range of nip load. It was also unfortunate as the type of computations involved are some of the most challenging for engineers and scientists to solve. Welp and Guldenberg [37] focused on various types of nip contact and recognized that to model a particular case that sub-models needed to be coupled. For instance in the majority of center winders with impinged nip rolls and surface winders the web contacts the nip roll with some angle of wrap prior to being wound onto the roll.

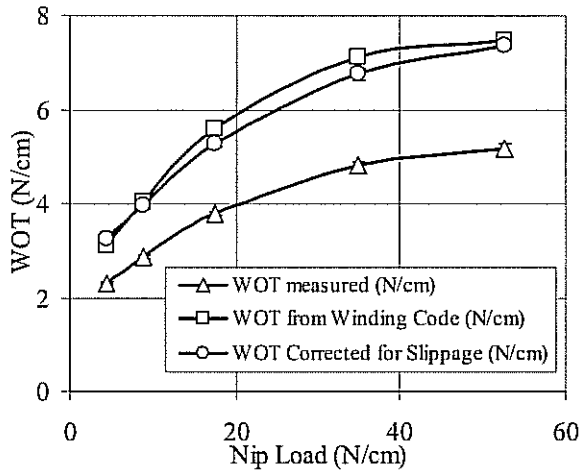

Figure 24- Good et al [36] WOT Data for Newsprint, Center Winding with an Undriven Nip Roller

This is a common practice whose origin is based on web instability, as the web approaches the winder it is preferable to first contact a roller which is cylindrical with all points on the roller surface moving at constant velocity. The degree to which the wound roll is cylindrical is affected by the uniformity of web thickness with respect to the cross machine direction that is presented to the winder and by the variation in nip load across the width of the wound roll. Thus it is preferable to have the web wrap the nip roll prior to contact with the wound roll to minimize web wrinkles and fold-overs that would have resulted from contacting a wound roll with non-uniform surface velocity first. For this case Welp and Guldenberg coupled models which govern stick and slip of the web upon the surface of the nip roll with models that account for the stick and slip in the nip contact zone. Jorkama and von Hertzen [38-40] were the first to develop a model for the WOT based upon a contact mechanics approach. This model required numerical solution but allowed the WOT to be studied as a function of nip and wound roll diameter, web material properties, the friction characteristics, winder operating parameters such as nip load and web tension, and whether one was center winding with a nip or surface winding. Good [41] focused on developing a closed form WOT model that did not require numerical solution. He accomplished this by enforcing assumptions regarding where slip could occur in the nip contact zone. He demonstrated the ability of this model to predict the WOT associated with center winding with an undriven nip roller on news print and polyester webs.

Some results from that study are shown in Figure 25 where the WOT has been measured and modeled for center winding newsprint with nip rolls of varied diameters. Items of interest include that at low nip loads the WOT is approaching the web tension (T_w) per expression {29} and that at higher nip loads it becomes less dependent on nip load. The results also show that smaller nip diameters appear to increase the range of nip load over which expression {29} is valid.

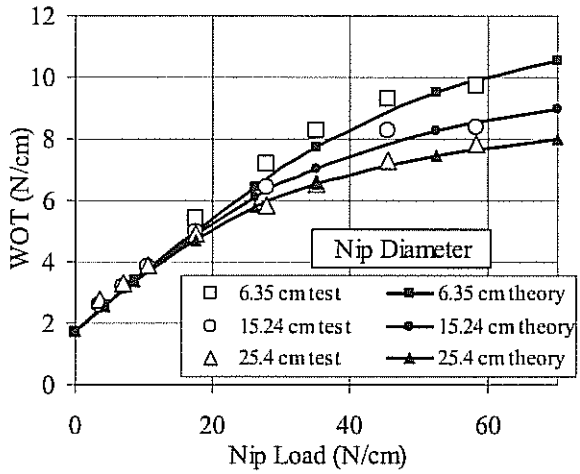

Figure 25 – Effect of Nip Roller Diameter on WOT when Center Winding Newsprint at a Winding Tension of 1.75 N/cm

WOT on Two Drum Winders. The WOT for multiple drum winders such as two drum winders has also been studied. The first experimental WOT data appeared in Rand and Eriksson [28] as previously mentioned, results of which appear in Figures 26a and 26b. The WOT appears to reach its highest value in the outer layer of the winding roll. Other strain data (not shown) indicated that the WOT increased with wound roll radius when the rider roll load was held constant at 17.5 N/cm. With two drum winders there is potential for induced slippage between the outer layer and the layer beneath at either of the two drum locations or beneath the rider roll impinged from above, see Figure 27. The contact points between the two drums and the wound roll move away from one another as the wound roll builds in radius. Thus setting the rider load to a constant does not mandate that the nip loads at the drums remain constant, in fact they vary due to the increased weight of the wound roll and the increasing distance between the wound roll contacts with the drums as the wound roll increases in outside radius.

Rand and Eriksson displayed results as well for a case where the rider load was reduced from 17.5 to 0 N/cm during winding. In this case the WOT was reasonably constant with wound roll radius but had they wound to greater wound roll radii the drum nip loads would have begun to increase dramatically due to the dead weight of the winding rolls. This would result in increased WOT from the drums which presumably would have ultimately resulted in a web burst, the bane of two drum winders. Olsen and Irgens [42,43] developed theoretical WOT algorithms for two drum winders which included dynamic terms and maximum bounds for the nip induced slippage, these algorithms were not verified by winding tests. Good et al. [44] studied two drum winding in depth in the laboratory. Winding trials were conducted on a two drum winder by two methods. The first method was that of Steves [35] described earlier which used pull tabs to measure the pressures and a winding model to infer what the WOT must have been to produce those pressures. The second method was that of Pfeiffer [29] applied to the two drum winder where the web was extracted from the surface of the wound roll between the first drum and the rider and was wrapped about an idler on mounted upon load cells to measure the WOT at that location. The web was extracted again from the surface from the wound roll between the rider roll and the second drum such to make a second WOT measurement as shown in Figure 27.

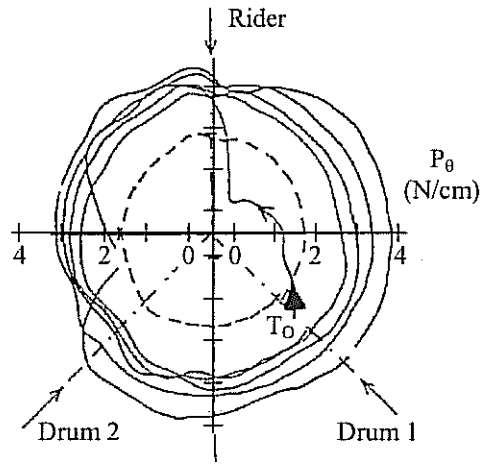

Figure 26a- Rand and Eriksson Circumferential Load Data acquired on Newsprint on a Two Drum Winder at a Wound Roll Radius of 10.2 cm. *(Reprinted with the permission of L.G. Eriksson)*

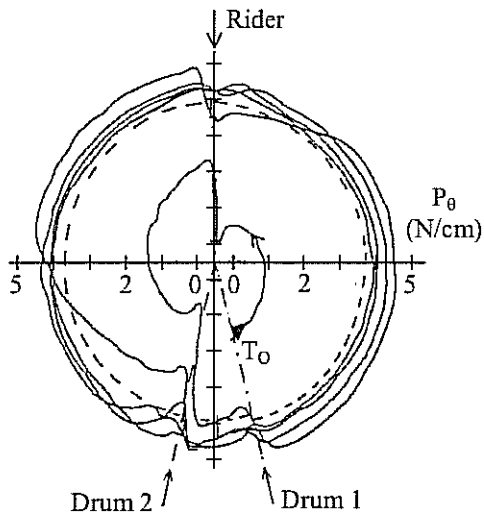

Figure 26b- Rand and Eriksson Circumferential Load Data acquired on Newsprint on a Two Drum Winder at a Wound Roll Radius of 78.7 cm. *(Reprinted with the permission of L.G. Eriksson)*

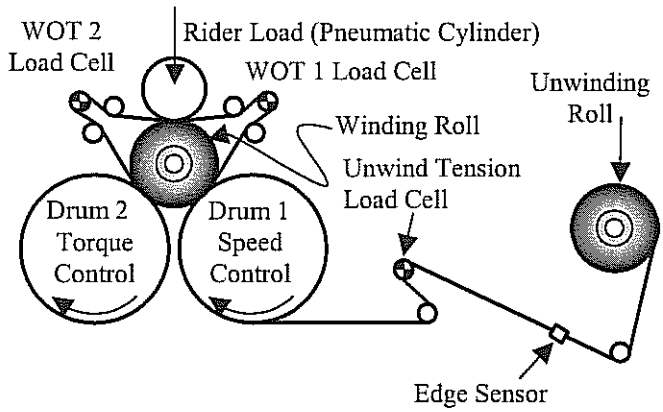

Figure 27 - Two Drum Winder WOT Measurement

For the thread path shown the results of the study proved that the incoming web tension to the winder had no impact on the WOT, the increased web tension was absorbed as an increased torque requirement required to maintain the first drum at constant velocity, refer to Figure 28. Thus increasing web tension prior to the winder had little or no effect on the wound roll pressures and stresses, but it would increase the probability of a web break prior to the winder. Note as well that the WOT inferred from measured pull tab pressures and winding models were in excess of the WOT measured directly with idlers on load cells, a second example that the extraction of the web from the wound roll surface interferes with the WOT which is being measured. Increasing the torque to the second drum resulted in proportionate increases in WOT as shown in Figure 29. Increasing the rider roll load resulted in significant increases in WOT as shown in Figure 30. This provides insight why the taper of rider load with wound roll diameter has been an effective practice in controlling the WOT. It should be noted that the thread path shown for the two drum winder in Figure 27 is but one of four possibilities. It is very tedious to wind rolls while inserting pull tabs and if one is simply studying the trend of WOT with respect to winder operating parameters the method of Pfeiffer [29] is very efficient. The pull tab method requires that entire rolls be wound at fixed levels of the winder operating parameters however several levels of winder operating parameters can be studied while winding one roll with Pfeiffer's method. The results show that some thread paths are more advantageous than others in that winder operating parameters such as incoming web tension and drum torque may have little impact on wound roll pressures and stresses leaving only the rider load as the only influential winder parameter [44].

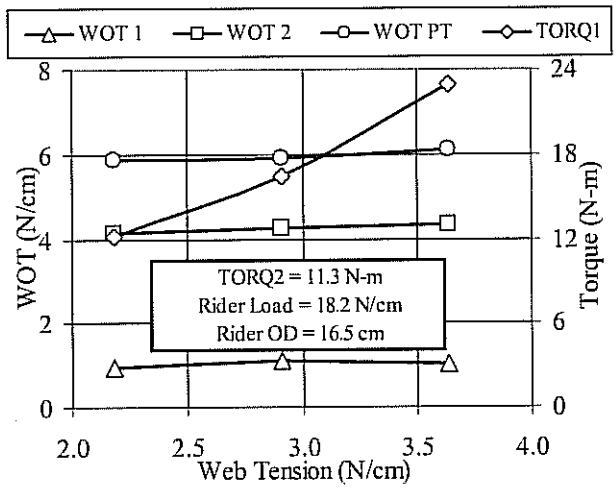

Figure 28 – Effect of Web Tension on WOT when Winding Newsprint on a Two Drum Winder

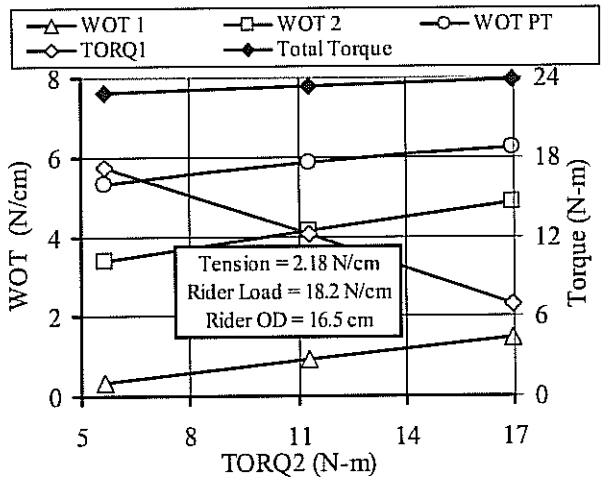

Figure 29 – Effect of Torque Input to Drum 2 on WOT when Winding Newsprint on a Two Drum Winder

WOT Summary. In summary it is known that the winding models which were reviewed are applicable to types of winders other than the center winding case for which the models were derived. If the WOT is known it can be substituted into expression {30} and with the core boundary conditions {15 or 24} the second order differential equations {11 or 22} can be solved to yield the increments in pressure that resulted from the addition of the last layers. Then expressions {16} and {17} can be used to track the total pressure and circumferential stress within the roll as a function of radius. It is currently difficult to determine what the WOT is for various winders. The simple WOT models for center winding with a rider roll {29} or for surface winding {31} may be applicable to a generic web but it is unknown for the generic web at what nip load stick behavior will commence in the contact zone and thus require use of the contact mechanics modeling methods described by Welp and Guldenberg, Jorkama and von Hertzen, and Good.

Although these models are described in the literature their implementation in coding is not insignificant.

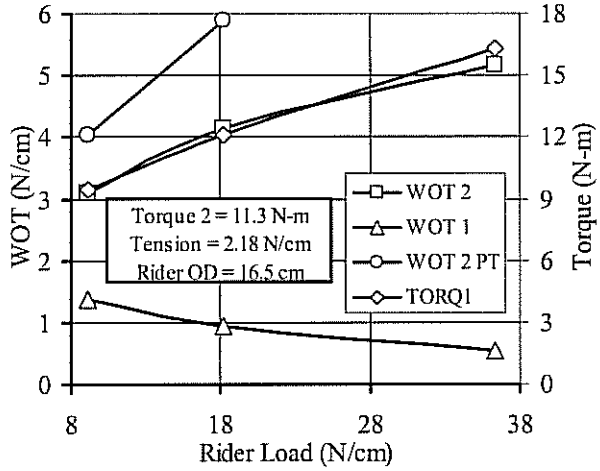

Figure 30 – Effect of Rider Roller Load on WOT when Winding Newsprint on a Two Drum Winder

WEB MATERIAL/ENVIRONMENTAL EFFECTS

To this point the web and the wound roll have been treated as an elastic material with constant in-plane modulus and a radial modulus (E_r) which is state dependent on pressure. In fact the in-plane modulus (E_θ) could be state dependent on the level of the circumferential stress as well in the second order differential equation in radial pressure {11}. Temperature and moisture content variation can cause the pressure and circumferential stresses to change from the as-wound values. Many web materials are viscoelastic, in that they may creep or contract through time. Pressures and circumferential stresses in rolls wound of viscoelastic webs will vary through time. Environmental effects such as moisture or temperature typically affect the rate of the behavior. In hygroscopic materials such as paper, the primary plasticizer may be moisture but the moisture level may be influenced by temperature.

The end result is through changes in temperature and moisture content and/or with passage of time substantial decrease or increases in pressures and circumferential stresses may occur. These increases in pressure can lead to roll defects and the decreases can result in a wound roll that cannot be successfully transported or unwound. In webs which have been wound after printing or some other process where registration is important, these influences can cause variation in registration as the roll is unwound in the converting process.

Thermoelastic and Hygroscopic Web Behavior

Tramposch [45] was the first in the literature to present a solution to the thermoelastic winding problem in 1967. Tramposch assumed that the wound roll was isotropic (E_r=E_θ). It was during this same time period that state dependency was discovered in the radial modulus [6]. Connolly and Winarski [46] presented a thermoelastic model in which orthotrophy was allowed in the moduli, but the state dependency on radial pressure of the radial modulus was not incorporated. Willett and

Poesch [8] developed a winding model very similar to that of Hakiel [7] which also incorporated the state dependency of the radial modulus but included thermoelastic terms in the development of the differential equation. Although thermoelasticity was treated in the development Willett and Poesch provided no verification of the thermoelastic portion of the model. Qualls and Good [47] presented a thermoelastic development that included the state dependency of the radial modulus on pressure and which was verified in the laboratory. In a thermoelastic winding model development the strains must now be defined as total strains which include the effects of temperature change and expressions {2} become:

$$\begin{aligned} \varepsilon_r &= \frac{\sigma_r}{E_r} - \frac{\nu_{r\theta}\sigma_\theta}{E_\theta} + \alpha_r \Delta T \\ \varepsilon_\theta &= \frac{\sigma_\theta}{E_\theta} - \frac{\nu_{\theta r}\sigma_r}{E_r} + \alpha_\theta \Delta T \end{aligned} \qquad \{32\}$$

The circumferential stress σ_θ can be eliminated from the strain expressions using the equilibrium expression {1}. Combining the total strain expressions {32} with the compatibility expression {9} yields:

$$\begin{aligned} &\frac{r^2}{E_\theta}\frac{\partial^2\sigma_r}{\partial r^2} + \left[\frac{3r}{E_\theta} - \frac{r\nu_{\theta r}}{E_r} + \frac{r\nu_{r\theta}}{E_\theta}\right]\frac{\partial\sigma_r}{\partial r} + \\ &\left[-\frac{r}{E_r}\frac{\partial\nu_{\theta r}}{\partial r} - r\nu_{\theta r}\left(-\frac{1}{E_r^2}\frac{\partial E_r}{\partial r}\right) + \frac{1+\nu_{r\theta}}{E_\theta} - \frac{1+\nu_{\theta r}}{E_r}\right]\sigma_r = \left(\alpha_r - \alpha_\theta\right)\Delta T \end{aligned} \qquad \{33\}$$

Next the temperature change is assumed to be uniform throughout the roll, Maxwell's expression {7} is incorporated, and the assumption that the in-plane modulus E_θ and the Poisson's ratio $\nu_{r\theta}$ are constants yields a simplified form:

$$r^2\frac{d^2\sigma_r}{dr^2} + 3r\frac{d\sigma_r}{dr} - \left(\frac{E_\theta}{E_r} - 1\right)\sigma_r = E_\theta\left(\alpha_r - \alpha_\theta\right)\Delta T \qquad \{34\}$$

Note the left hand side of this expression is identical to expression {10}. Two boundary conditions are required to solve this expression. One boundary condition is obtained again by enforcement of displacement compatibility at the core but now the total deformation of the outside of the core, including thermal deformation, must be equal to the total deformation of the inside of the first layer:

$$\begin{aligned} u_{core} &= u_{layer1} \\ \frac{\sigma_r}{E_c} + \alpha_c \Delta T &= \varepsilon_\theta \end{aligned} \qquad \{35\}$$

The constitutive expressions {32} and the equilibrium expression {1} can be used to cast this boundary condition in terms of σ_r:

$$r_c\left.\frac{d\sigma_r}{dr}\right|_{r=r_c} + \left(1 - \nu_{r\theta} - \frac{E_\theta}{E_c}\right)\sigma_r\Big|_{r=r_c} = E_\theta\left(\alpha_c - \alpha_r\right)\Delta T \qquad \{36\}$$

The second boundary condition results from surface equilibrium at the outside of the outermost layer of the wound roll:

$$\sigma_r\Big|_{r=outside\_radius} = 0 \qquad \{37\}$$

This derivation assumes that the environmental changes during winding are inconsequential. It also assumes that the wound roll is at a uniform temperature initially

and that either due to heating or cooling conditions the roll temperature changes to a new value but remains uniform throughout the roll. Thus this model should not be used to study transient conditions where the temperature at the outside of the roll may differ from that inside the roll. The thermoelastic model differs from the winding models described earlier in that the thermoelastic model is used to study variations in pressure and circumferential stress within the roll after winding has been completed. Thus this is not an accretive solution but is a boundary value problem. Use of the thermoelastic model requires that a winding model was already exercised such that the pressures and circumferential stresses due to winding at a reference temperature are already known. Thus the radial modulus (E_r) as a function of radius is known at the start of the thermoelastic solution. The change in temperature for the thermoelastic model is calculated with respect to the reference temperature at the time of winding. Even though the thermoelastic model does not involve accretive solutions, the solution should occur over several steps because of the state dependency of the radial modulus on pressure. The thermal coefficients of expansion (α_θ, α_r, and α_c) must be known to exercise a thermoelastic solution and often require measurement. The radial thermal expansion coefficient of a stack of web (α_r) is not a property to be found in a reference and will require measurement. The thermal expansion coefficient of a core (α_c) may exist in a reference if the core is composed of metal however the coefficient for a fiber core will require measurement. To illustrate the possibilities, an example of winding a 64 μm thick polyethylene web is given for a winding tension of 620 KPa. The measured web and core properties are provided in Table 2.

Web Properties		Core Properties	
E_θ	172 MPa	E_c	19 GPa
E_r	K_2=167	α_c	$1.08*10^{-5}$ m/m/°C
α_θ	$3.35*10^{-4}$ m/m/°C	Winder Parameters	
α_r	$1.01*10^{-4}$ m/m/°C	T_w	620 KPa

Table 2 – Data for Center Winding Polyethylene.

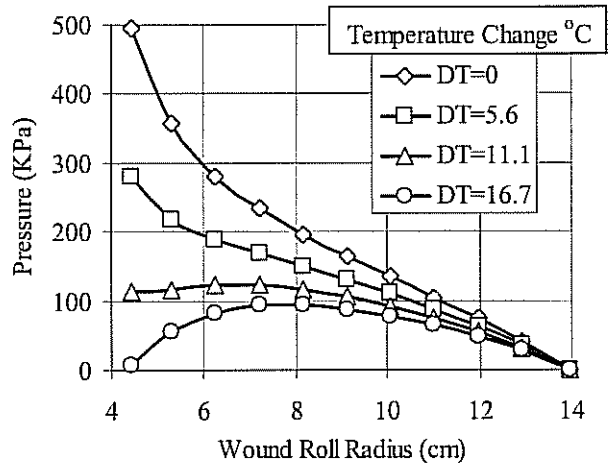

Figure 31 – Radial Pressures within Rolls Wound from 64 μm Polyethylene at the Winding Temperature and Elevated Temperatures

The radial pressures and circumferential stresses are presented for winding the roll at ambient temperature, and then as a result of temperature increases of 5.6, 11.1, and

16.7°C after winding in Figures 31 and 32, respectively. At the highest increase in temperature note that all pressure has been lost at the core which may result in a loose core or problems with core slippage at the next unwind. Also note that the circumferential stresses at the core moved from 620 KPa just after winding to -310 KPa after a temperature increase of 16.7°C. Circumferential buckles in the web near the core may now be possible.

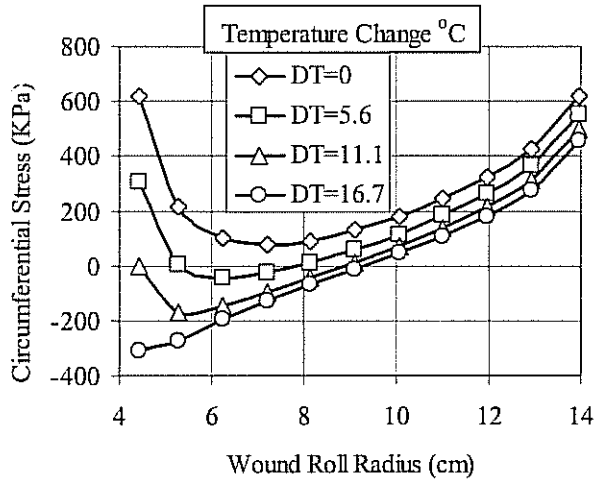

Figure 32 – Circumferential Stresses within Rolls Wound from 64 μm Polyethylene at the Winding Temperature and Elevated Temperatures

Many paper webs are quite hygroscopic and as such their dimensions are affected by the amount of moisture which is present in the web. If the moisture content of a wound roll of paper changes through time changes in outer diameter and pressure and internal circumferential stresses can be expected [48]. The analysis of hygroscopic activity and thermoelastic activity within wound rolls is nearly identical. The total strain expressions {32} which were presented for the thermoelastic analysis are modified to account for dimensional changes resulting from changes in moisture content:

$$\varepsilon_r = \frac{\sigma_r}{E_r} - \frac{\nu_{r\theta}\sigma_\theta}{E_\theta} + \beta_r \Delta H$$
$$\varepsilon_\theta = \frac{\sigma_\theta}{E_\theta} - \frac{\nu_{\theta r}\sigma_r}{E_r} + \beta_\theta \Delta H \qquad \{38\}$$

where the β_r and β_θ are the hygroscopic coefficients of expansion in the radial and tangential directions, respectively, and ΔH is the change in moisture content. The product of $\beta\Delta H$ must be dimensionless and thus the units of β and ΔH need chosen accordingly. Similarly the core boundary condition becomes:

$$r_c \left.\frac{d\sigma_r}{dr}\right|_{r=r_c} + \left(1 - \nu_{r\theta} - \frac{E_\theta}{E_c}\right)\sigma_r\Big|_{r=r_c} = E_\theta(\beta_c - \beta_r)\Delta H \qquad \{39\}$$

The outer boundary condition {37} is unchanged. The solution method and limitations are similar to that described for the thermoelastic analysis. Paper webs are hygroscopic but since moisture is the primary plasticizer it is difficult to separate the hygroscopic and viscoelastic response of the web. Thus it could be argued that a model that captures only

the hygroscopic response is more of an academic curiosity than a useful tool for paper webs.

Viscoelastic Behavior

In viscoelasticity the strain behavior through time is no longer constant, even under constant stress. Viscoelasticity is important within wound rolls as it can cause the pressures to increase or decrease with time rather than with respect to environmental effects such as moisture and temperature changes which have already been discussed. There are also combined influences. For instance an increase in moisture in a wound roll of paper or an increase in temperature in a wound roll of plastic film will increase the rate at which the viscoelastic deformation occurs.

Transient analysis of wound roll stresses was first modeled by Tramposch [45,49] who modeled viscoelastic web behavior using a Maxwell-Kelvin constitutive law. Tramposch first [49] modeled the web in the wound roll as an isotropic viscoelastic material but later [45] extended his model to allow the study of orthotropic viscoelastic materials by allowing the radial and circumferential moduli to differ by a multiplicative constant. Lin and Westman [50] incorporated viscoelastic effects during the time required to wind the roll and modeled the web in the roll as an isotropic viscoelastic material using a generalized Maxwell model. Qualls and Good [51] modeled the web in the wound roll as an orthotropic viscoelastic material using generalized Maxwell constitutive laws and allowing state dependency in the radial modulus.

The strains are now related to creep functions (J) and rates of change of stresses through time as:

$$\begin{aligned}\varepsilon_r &= \int_0^t \left[J_r(t-t')\frac{\partial \sigma_r}{\partial t'} + J_{r\theta}(t-t')\frac{\partial \sigma_\theta}{\partial t'} \right] dt' \\ \varepsilon_\theta &= \int_0^t \left[J_\theta(t-t')\frac{\partial \sigma_\theta}{\partial t'} + J_{\theta r}(t-t')\frac{\partial \sigma_r}{\partial t'} \right] dt'\end{aligned} \qquad \{40\}$$

where the creep functions J are determined by experiment in the generalized Maxwell form:

$$J\left(t-t'\right) = J_0 + \sum_{i=1}^{N} J_i e^{-\left(t-t'\right)/\tau} \qquad \{41\}$$

Combining these expressions for the strain {40} with the equilibrium expression {1} and the strain compatibility equation {9} leads to the following integral boundary value problem written in terms of a second order partial differential equation in terms of the radial stress, radius, and time:

$$\int_0^t \left[\begin{array}{l} J_\theta\left(t-t'\right)\dfrac{\partial}{\partial t'}\left(r^2 \dfrac{\partial^2 \sigma_r}{\partial r^2} \right) + \\ \left\{ 3J_0\left(t-t'\right) + J_{\theta r}\left(t-t'\right) - J_{r\theta}\left(t-t'\right) + r\dfrac{\partial}{\partial r}\left(J_\theta\left(t-t'\right) \right) \right\} \dfrac{\partial}{\partial t'}\left(r\dfrac{\partial \sigma_r}{\partial r} \right) + \\ \left\{ \begin{array}{l} r\dfrac{\partial}{\partial r}\left(J_\theta\left(t-t'\right) + J_{\theta r}\left(t-t'\right) \right) + \\ J_\theta\left(t-t'\right) + J_{\theta r}\left(t-t'\right) - J_r\left(t-t'\right) - J_{\theta r}\left(t-t'\right) \end{array} \right\} \dfrac{\partial \sigma_r}{\partial t'} \end{array} \right] dt' = 0 \qquad \{42\}$$

Two boundary conditions are required to solve this expression through time. Displacement compatibility between the core and the inner layer of web provide one of the boundary conditions:

$$\frac{(\sigma_r)_j\Big|_{r=r_c}}{E_c} = (\varepsilon_\theta)_j\Big|_{r=r_c} \qquad \{43\}$$

where the subscript j denotes the values of the variables at time t_j. The second boundary condition involves the outermost lap. Tramposch employed surface equilibrium on the outside surface of the outermost lap which yields that the radial pressure at that location should be zero for all time. This is a satisfactory condition for models that do not account for the state dependency of material properties. Lin and Westman employed a boundary condition that forced the circumferential stress in the outermost layer to be constant through time. This would seem questionable since in many cases the outer layer is subject to the highest circumferential stress in the wound roll and thus most apt to relax as a function of the in-plane relaxation J_θ. Qualls and Good employed an outer boundary condition that allowed the circumferential stress to decay in the outer layer but forced the circumferential strain (ε_θ) to be constant throughout time. Although at first this may seem as unreasonable as Lin and Westman's outer boundary condition recall that in axisymmetry that the circumferential strain is defined as the radial deformation (u) divided by the radius {8}, so Qualls and Good's boundary condition is also a statement that the deformation of the outer surface of the wound roll is negligible throughout time:

$$T_w J_\theta(0) = \int_0^t \left[J_\theta(t-t')\frac{\partial \sigma_\theta}{\partial t'} + J_{\theta r}(t-t')\frac{\partial \sigma_r}{\partial t'} \right] dt' \qquad \{44\}$$

Earlier the measurement of the Poisson ratio $\nu_{\theta r}$ was discussed. It was shown to be state dependent on pressure but small. Thus it is logical that the creep function terms such as $J_{\theta r}$ and $J_{r\theta}$ are small compared to the J_r and J_θ terms and as a result they are typically neglected in application. Thus expression {42} condenses to:

$$\int_0^t \left[\begin{array}{l} J_\theta\left(t-t'\right)\dfrac{\partial}{\partial t'}\left(r^2\dfrac{\partial^2\sigma_r}{\partial r^2}\right) + \\ \left\{3J_\theta\left(t-t'\right) + r\dfrac{\partial}{\partial r}\left(J_\theta\left(t-t'\right)\right)\right\}\dfrac{\partial}{\partial t'}\left(r\dfrac{\partial\sigma_r}{\partial r}\right) + \\ \left\{r\dfrac{\partial}{\partial r}\left(J_\theta\left(t-t'\right)\right) + J_\theta\left(t-t'\right) - J_r\left(t-t'\right)\right\}\dfrac{\partial\sigma_r}{\partial t'} \end{array} \right] dt' = 0 \qquad \{45\}$$

which is subject to simplified boundary conditions:

$$\begin{aligned} \frac{(\sigma_r)_j}{E_c} &= (\varepsilon_\theta)_j \\ T_w J_\theta(0) &= \int_0^t \left[J_\theta(t-t')\frac{\partial \sigma_\theta}{\partial t'} \right] dt' \end{aligned} \qquad \{46\}$$

To apply these models requires knowledge of radial and circumferential moduli, the core stiffness, the creep functions and knowledge of the stress state of the wound roll at the end of winding. This stress state could be determined from elastic winding models which were discussed earlier.

The impact of viscoelasticity can be very significant on wound roll stresses. As an example some results will be presented for a paper tissue web. The J_θ creep test data is obtained by subjecting the web to a machine direction stress and then recording the machine direction displacement and strain behavior through time. These tests are repeated for several stress levels. Results from these tests are shown in Figure 33. The elastic strains are subtracted from the total strain data leaving only the viscoelastic strain through time. This strain data is then normalized by dividing by the applied stress level at that point all of this data collapses to one curve which is indicative of a linear viscoelastic material. A curve fit of the form of expression {41} is then performed which resulted in the following creep function:

$$J_\theta(t) = 0.000319 - .000102e^{-t/4} - .000102e^{-t/100} - .000116e^{-t/1000} \quad t(\text{min}) \qquad \{47\}$$

where time (t) has units of minutes. The total strain for a constant stress can then be predicted through time using the expression:

$$\varepsilon_\theta(t) = J_\theta(t)\sigma_0 + \frac{\sigma_\theta}{E_\theta} \qquad \{48\}$$

The accuracy of expression {48} is shown by the curve fits at the various applied stress levels in Figure 33.

The J_r creep test data is determined in a similar fashion except now a stack of web is subjected to pressure whilst recording the normal displacement and strain behavior through time. In this case the test is repeated for several applied stack pressures and the data is shown in Figure 34. Again the elastic strains are subtracted from this data and then the data is normalized by dividing by the test stack pressure. Again the data collapse to one curve which is fit by an expression of the form of expression {41}:

$$J_r(t) = 0.001597 - .00044e^{-t/10} - .00044e^{-t/100} - .00073e^{-t/1000} \quad t(\text{min}) \qquad \{49\}$$

The total strain for a constant pressure P can then be predicted through time using the expression:

$$\varepsilon_r(t) = J_r(t)P + \frac{P}{E_r} \qquad \{50\}$$

The accuracy of expression {50} is demonstrated by the curve fits at the various applied stack pressure levels in Figure 34.

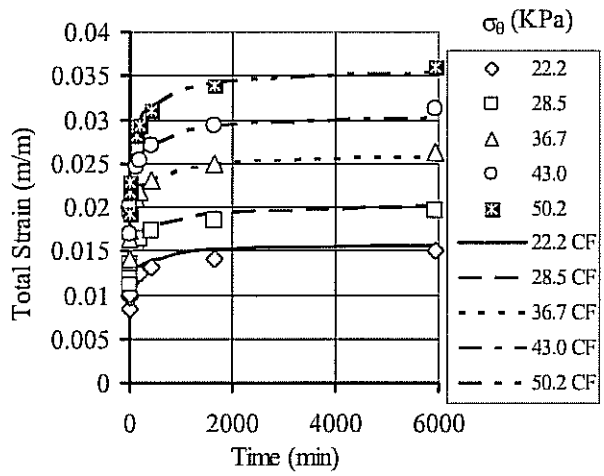

Figure 33 – Total In-Plane Strain in a Paper Tissue Web through Time at Various Stress Levels and Curve Fits per Expressions {47 & 48}

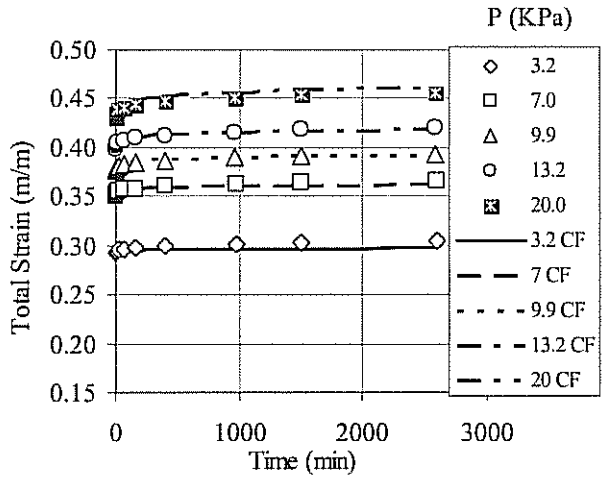

Figure 34 – Total Normal Strain in a Stack of Paper Tissue Web through Time at Various Applied Pressure Levels and Curve Fits per Expressions {49 & 50}

Web Properties		Core Properties	
E_θ	3.34 MPa	E_c	30 GPa
E_r	K_1=0.258 KPa	Winder Parameters	
	K_2=13.5	T_w	150 KPa

Table 3 – Data for Winding Paper Tissue.

These creep functions along with the other parameters in Table 3 were used to study how the pressures and stresses varied with rolls of tissue through time. The rolls were wound at a constant winding tension of 150 KPa. The internal roll pressures and circumferential stress predicted by Qualls' model [51] are shown at 3 instants in time in Figures 35 and 36, respectively.

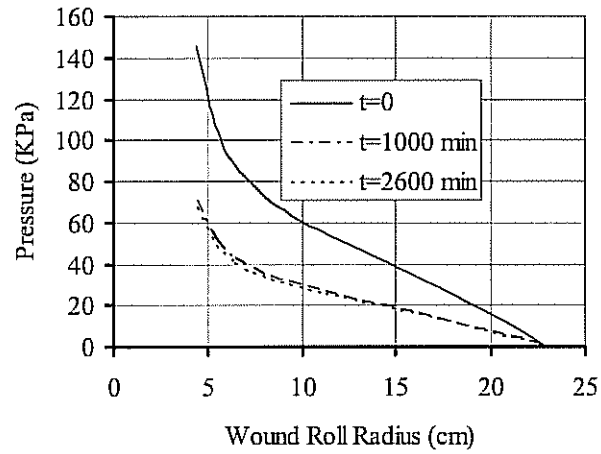

Figure 35 – Pressure Decay in Tissue Rolls Center Wound at a Winding Tension of 150 KPa

The significance of viscoelasticity is demonstrated in noting that between the time at which the roll was wound (t=0 min) and 1000 minutes later that essentially half the pressure has been lost in the roll. But very little loss in pressure is noted between 1000 and 2600 minutes after winding, which is expected since the largest time constant in the creep expressions {47 & 49} is 1000 minutes. After 1000 minutes the roll has become viscoelastically "dead" and the pressure and circumferential stress will only change minutely thereafter.

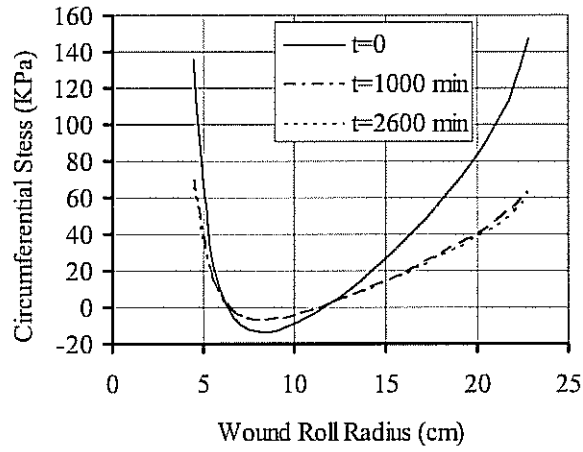

Figure 36 – Circumferential Stress Decay in Tissue Rolls Center Wound at a Winding Tension of 150 KPa

For polymeric and metal webs the rate at which creep occurs will be affected by changes in temperature. Creep will occur more readily at temperatures which are in excess of the winding temperature and creep will be restricted when the storage temperature is less than the winding temperature. If in fact the storage temperature is less than the glass transition temperature, creep will cease altogether. The effect of temperature on viscoelastic behavior within wound rolls has been modeled and verified by Qualls [48].

AIR ENTRAINMENT

Amplitude of the Entrained Air

Center Winding. Blok and VanRossum [52] developed a foil bearing relationship that predicted the thickness of a air lubricating film that forms between webs and rollers. Knox and Sweeney [53] verified this expression through friction tests and knowledge of the asperity heights upon a web surface. For the geometry and boundary conditions of Figure 37a the minimum air film thickness was determined from hydrodynamic theory as:

$$h_o = 0.643\ R \left[\frac{6\eta\left(V_{web} + V_{roller}\right)}{T} \right]^{2/3} \qquad \{51\}$$

where η is the viscosity of air which varies with process temperature $\left(\eta = 1.85 * 10^{-6}\ N - sec/m^2\ @25^\circ C\right)$. This expression is familiar to those who coat

webs where η is now the viscosity of the coating and often the web is coated over a stationary dead bar such that V_{roller} is set to zero. As webs pass over rollers subject to conditions of good traction, the web and roller velocities are nearly the same. The velocities of the incoming web and the surface of the winding roll are nearly the same such that expression {51} can be simplified to:

$$h_o = .643\, R \left[\frac{12\eta V}{T}\right]^{2/3} \qquad \{52\}$$

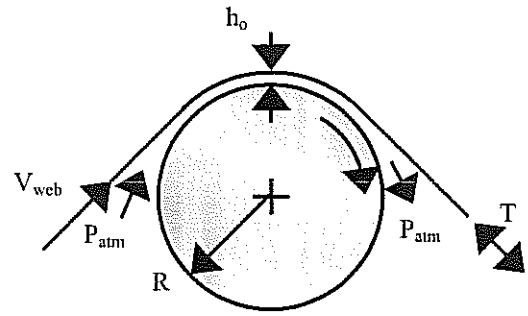

Figure 37a – Air Films Entrained between Webs and Rollers.

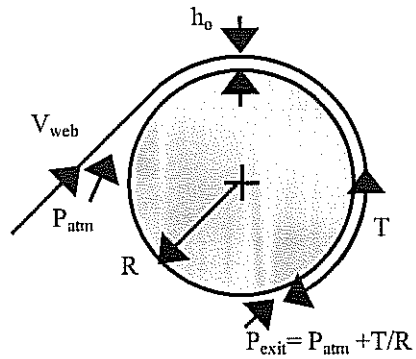

Figure 37b – Air Entrainment in Center Winding

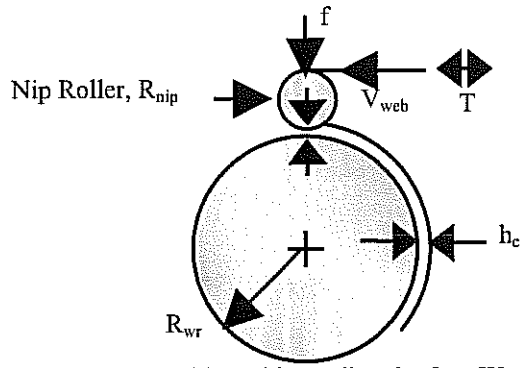

Figure 37c - Rolls Center Wound with a Rider Roll or Surface Wound Rolls where the Web First Wraps the Nip Roller

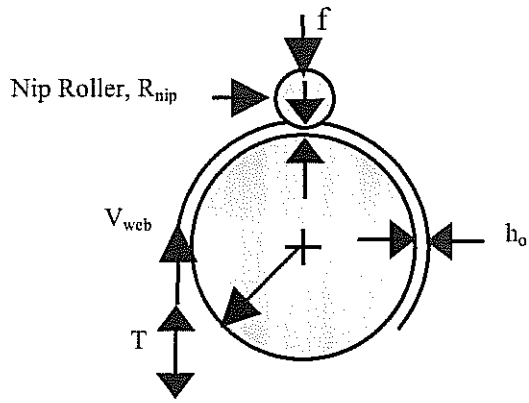

Figure 37d - Rolls Center Wound with a Rider Roll or Surface Wound Rolls where the Web First Wraps the Wound Roll

Connolly and Winarski [46] surmised that expression {52} was applicable to center winding rolls. The geometry and boundary conditions of the outer lap of a center winding roll is shown in Figure 37b, note the only difference is the absolute pressure at the exit which has become the sum of the atmospheric pressure and the equilibrium pressure beneath the outer lap of a winding roll. For many webs such as papers and plastic films, the web tension may vary in the range of 0.1 to 5 N/cm (load per unit width). The largest component of the exit pressure due to web tension would be seen near the core. For a core 5 cm in outer radius and a web tension of 5 N/cm this results in a total exit pressure about 10% greater than atmospheric pressure. For the majority of cases the exit pressure will be very nearly atmospheric pressure at which point the geometry and boundary conditions become identical to those shown in Figure 37a and it would be assumed the air film thickness expression {52} would be applicable.

Holmberg and Good provided proof that expression {52} was applicable to center winding rolls by pulsing and air jet normal to the outer layer of the winding roll and measuring the out-of-plane movement of the web with a reflected laser light transducer [54]. To ensure that entrained air beneath layers 2, 3 and below were not measured a nip roll was impinged into the winding roll just before the outer layer became layer 2. Taylor and Good [55] performed additional measurements in which the edges of wound rolls of polyester film were sealed with wax during winding. These rolls were subsequently unwound under water and the air which had been entrained was captured and the volume was measured. The volume divided by the total length of web wound into the roll and the roll width provided an average value of the entrained air film thickness in the wound roll. These values compared nicely with expression {52} as shown in Figure 38 and thus expression {52} was deemed valid for estimating the entrained air film during center winding.

There is evidence that a reduction in the air film can be realized with a precision dam that excludes the air at the entry point [56].

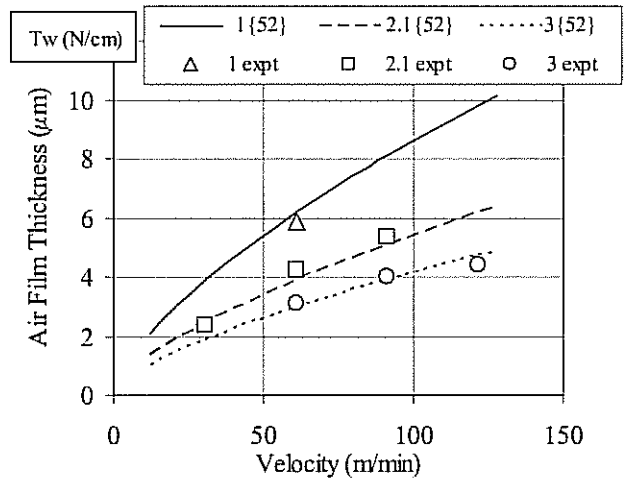

Figure 38 – Air Film Thickness for Center Winding at Varied Winding Tension and with a Average Wound Roll Radius of 5.72 cm

Center Winding with a Rider Roll or Surface Winding. A nip roller in contact with a wound roll can be very effective in excluding air before it is wound into a roll, note Figure 37c. Early treatments of the entrained air film thickness were based on hydrodynamic theory [57]:

$$f = 4\eta V\frac{R_e}{h_o} + \frac{4}{3\pi}\frac{T\sqrt{2R_e h_o}}{R_{wr}} \quad \text{where} \quad \frac{1}{R_e} = \frac{1}{R_{wr}} + \frac{1}{R_{nip}} \qquad \{53\}$$

and T is the web tension and f is the nip load, both in units of load per unit width. For inputs which are practical for paper and plastic webs the second term in expression {53} will be found insignificant compared to the first term, thus the expression can be rearranged as an expression for air film thickness. A later treatment was based on elastohydrodynamic theory. Chang [58] simultaneously solved the Reynolds and elasticity equations numerically to obtain solutions for the minimum air film thickness (h_o) and the final air film thickness (h_c) which results after the outer layer passes beneath the nip, note Figure 37c. The nip compresses the entrained air which expands to a larger value after exit of the nip as the pressure outside the outer layer decreases to atmospheric pressure. Chang's expression for the final air film thickness is:

$$h_c = \begin{cases} 7.4R_e\left(\dfrac{\eta V}{p_{atm}R_e}\right)^{0.66}\left(\dfrac{f}{p_{atm}R_e}\right)^{-0.21}\left(\dfrac{E}{p_{atm}}\right)^{-0.33} & \text{for } 0.69 \le E \le 4.84 \text{ MPa} \\ 12.5R_e\left(\dfrac{\eta V}{p_{atm}R_e}\right)^{0.71}\left(\dfrac{f}{p_{atm}R_e}\right)^{-0.20}\left(\dfrac{E}{p_{atm}}\right)^{-0.23} & \text{for } 4.84 \le E \le 34.5 \text{ MPa} \end{cases} \qquad \{54\}$$

where the combined modulus is defined as: $E = \dfrac{1}{\dfrac{1-\nu_r^2}{E_r} + \dfrac{1-\nu_{nip}^2}{E_{nip}}}$ {55}

This expression {54} produces air layers much larger than the hydrodynamic expression {53} for similar inputs. Taylor and Good [55] conducted experiments similar to those

described previously where the roll edges were sealed during winding (with a nip roller in this case) and then unwound under water where the air that had been entrained during winding was collected. Results shown in Figure 39 verify the applicability of expression {54} to winding rolls in the setup shown in Figure 37c and also that elastohydrodynamic theory is required to accurately model the entrained air layer thickness. It should be noted that these equations {53,54} do not account for the presence of the outer layer of web in the analysis, the original model considers two dissimilar rollers in contact one of which represents the winding roll. The experimental tests confirmed that the air is entrained beneath the outer layer and into the winding roll is well described by {54}. It should be noted that if the web wraps the wound roll first rather than the nip roller (Figure 37d), that the effectiveness of the nip roller in reducing the entrained air layer can be lost. In that geometry the air film beneath the outer layer may approach the level given by expression {52} for center winding, then decrease momentarily as the air compresses beneath the nip roller, and finally returns to the level given by expression {52}. It is also possible that the web will form a bubble immediately in front of the nip and the air will vent laterally through the bubble. This "bubble" in the web is typically unstable and may intermittently be drawn into the nip causing web creases. From the standpoint of web wrinkling it is advisable to allow the web to contact the roller first which is a more perfect cylinder, usually the nip roller is more so than the wound roll.

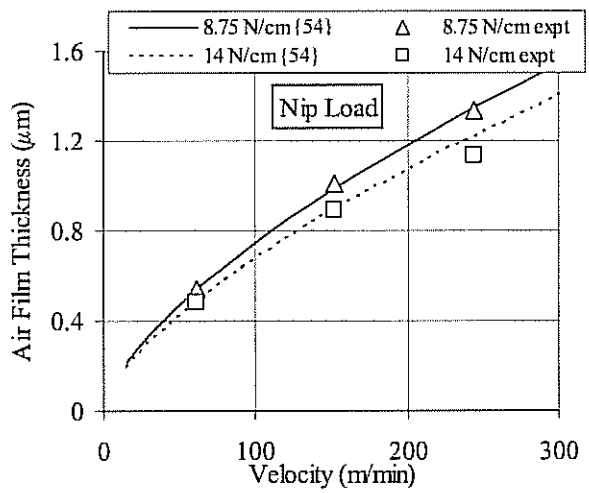

Figure 39 – Air Film Thickness for Center Winding with a Nip Roller, R_{nip} = 5.1 cm, $R_{wr,average}$ = 5.72 cm, and a Wound Roll Radial Modulus of 0.69 MPa.

Exhaust of Entrained Air

The air film may exhaust rapidly out the ends of the wound roll or in fact remain in the roll for long periods of time. The time required for the air film to decay from the original height (h_o) to some lesser height (h_f) at a given wound roll pressure (P) is related to the squared width (W) of the wound roll through the squeeze film expression presented by Blevins [59]:

$$t = \frac{\eta W^2}{2P}\left(\frac{1}{h_f^2} - \frac{1}{h_o^2}\right) \qquad \{56\}$$

Through this equation one can find that the time required for the entrained air thickness to decay from the initial value, per expressions {52} or {54}, to a final value at which the web surfaces begin to contact may require a few seconds or a few days depending on the web width, the pressure, and the initial air film thickness. Expression {56} was derived for the situation of a squeeze film damper where two plates which are parallel are being pushed together by a pressure P. The wound roll is much more complex due to multiple layers exhausting and the winding pressures at various radii being responsible for that exhaust, Keshavan and Wickert attack this problem [60].

Effect of Air Entrainment on Wound Roll Stresses

The effect of entrained air is multifaceted with regard to wound roll stresses. In general the effect of the entrained air is to reduce the wound roll pressure, the degree of which depending on how much air was entrained. One facet is the impact of the entrained air on the radial modulus (E_r). When the radial modulus was first presented in expressions {4} and {5} the state dependency on pressure was assumed to be due to asperity contact between web surfaces. The entrained air acts to reduce asperity contact at a given pressure. In their work on entrained air in center winding with a rider roller, Good and Covell [61] postulated that there were three realms in the expression for the radial modulus:

$$E_r = K_2\left(P + K_1\right) \qquad \text{when } h_o \le R_{q,eq}$$

$$E_r = \frac{h_o + h}{\dfrac{h}{K_2\left(P + K_1\right)} + \dfrac{h_o\left(P_o + P_{atm}\right)}{\left(P + P_o + P_{atm}\right)^2}} \qquad \text{when } R_{q,eq} \le h_o \le 3R_{q,eq} \qquad \{57\}$$

$$E_r = \frac{\left(P + P_o + P_{atm}\right)^2}{\left(P_o + P_{atm}\right)} \qquad \text{when } h_o \ge 3R_{q,eq}$$

where $R_{q,eq}$ is the equivalent root mean square roughness of the upper and lower surfaces of the web which is calculated per:

$$R_{q,eq} = \sqrt{R^2_{q,\text{ upper surface}} + R^2_{q,\text{ lower surface}}} \qquad \{58\}$$

A center winding model, of the type described earlier first derived by Hakiel, can be used to examine the effects of air entrainment on wound roll stresses [54]. The results of modeling and experimental winding tests on a polyester web 50.8 μm in thickness are shown in Figure 40. The modeled web material input data is shown in Table 4. It is evident the effect of air entrainment can be substantial, with the roll pressure dropping by a factor of four at a web velocity of 76 m/min. The pressure test data in Figure 40 were recorded just after winding. As the air begins to exhaust the internal roll pressures will decrease further. Bouquerel and Bourgin [62] and Forrest [63] also developed wound roll models that incorporated the effect of air entrainment through a modification of the radial modulus but also incorporated the assumption of plane strain in their analyses. Lei et al [64] derive a more elaborate expression for the effect of entrained air on the radial modulus and combine the effects of air entrainment and thermal variation in a study of wound roll stresses at the time of winding and later in storage.

Another facet of the entrained air is the decrease in the apparent coefficient of friction. As the entrained air separates the web surfaces there is less asperity contact and hence less normal force making the apparent coefficient of friction decrease. In the limit as the entrained air fully separates two web surfaces, the apparent coefficient of friction approaches zero as only the viscosity of air can react any shearing between the two

surfaces. This is important in the case of center winding with a nip as the WOT will be affected per expression {29} and for surface winding where a simple WOT expression was presented {31}. Thus the WOT can be appreciably decreased with increases in the air film thickness which will result in decreases in the internal roll pressures.

Web Properties		Core Properties	
E_θ	4.13 GPa	E_c	33 GPa
$E_{r,stack}$	K_1=0.1 KPa	Winder Parameters	
	K_2=301.3	T_w	6.89 MPa
R_q	1.62 μm		

Table 4 – Data for Center Winding Polyester.

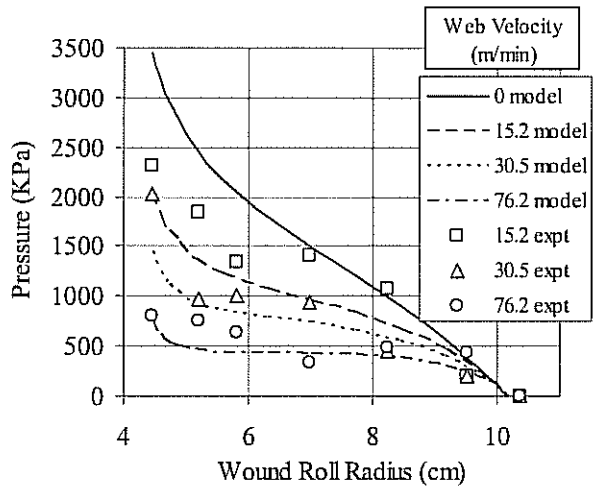

Figure 40 – The Effects of Air Entrainment on Roll Pressure when Center Winding Polyester at a Winding Tension of 6.89 MPa with the Properties stated in Table 4.

Effect of Air Exhaust on Wound Roll Stresses

As air exhausts from a wound roll, the internal roll pressures will decay. Each layer in the wound roll is similar to a balloon which is leaking air, mostly at the roll edges. The wound roll can have thousands of layers which could be envisioned as nested balloons all with air escaping at the edges at a rate dependent upon the radial pressure due to winding at that radius and the width of the roll per expression {56}. The decay of the air films within the roll results in a relaxation of the internal stresses within the roll. Taylor [65] found that a viscoelastic winding model could be used to study the decay of pressure in wound rolls as air exhausted from the rolls. Taylor accomplished this by determining a radial creep function ($J_r(t)$) based upon rate of air escape. Results for a polyester web 15.2 cm wide and 50.8 mm in thickness are shown in Figure 41, the web material and winder parameters are shown in Table 5. Please note that the pressures are very low, which is indicative of little or no contact between web surfaces. Also note that what pressure does exist in this narrow roll is decaying rapidly. Lei et al [64] discuss this as well. Many webs are permeable and thus exhaust of air is possible in the radial direction as well [66].

Web Properties		Core Properties	
E_θ	3.59 GPa	E_c	33 GPa
E_r	100 KPa	Winder Parameters	
J_r	$0.82-0.51e^{-t/100}-0.31e^{-t/1700}\ t(\text{sec})$	T_w	3.44 MPa
R_q	6.91 nm		

Table 5 – Data for Center Winding Polyester.

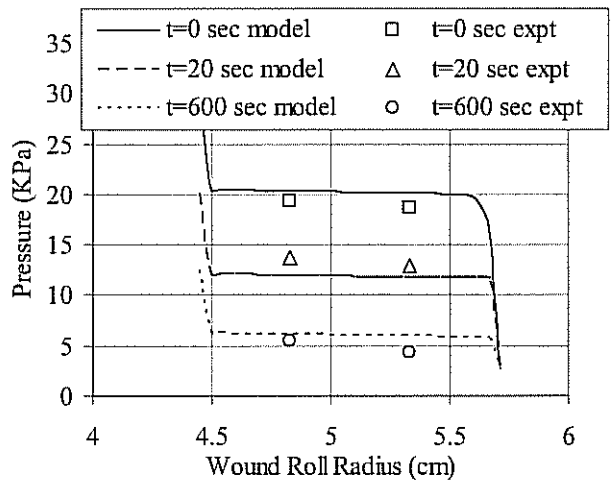

Figure 41 – Pressure Decay in a Center Wound Roll of Polyester Wound at 91.4 m/min with a Winding Tension of 3.45 MPa.

DYNAMICS

The velocity of webs wound into rolls has some variation through time depending on the winder hardware. The web velocity results in an angular velocity of the winding roll which will vary even if the web velocity is maintained constant. The angular velocity of the winding roll can produce centrifugal forces that can affect the internal stresses in a winding roll. Yagoda [67] studied this problem assuming the radial modulus (E_r) could be treated as a constant. He developed expressions which accounted for the total stresses during winding including the centrifugal effects and then additional expressions which allowed him to predict how the winding stresses would change when the wound roll was decelerated and finally stopped. Yagoda [68] applied these expressions to study how the stresses in newsprint rolls were affected by centrifugal forces. Yagoda concluded that the net effect on the stresses in the wound roll was virtually nil for the newsprint he studied up to velocities of 1200 m/min.

Olsen [69] formed an elasticity solution similar to that of Hakiel [7] but incorporated body force terms to account for forces due to centrifugal acceleration during the accretive process of winding.

$$r^2\frac{d^2(\delta P)}{dr^2}+3r\frac{d(\delta P)}{dr}+\left(1-\frac{E_\theta}{E_r}\right)\delta P=(3+\nu)\rho\delta\left(\frac{V^2}{s^2}\right)r^2 \qquad \{59\}$$

where ρ is the mass density and $\delta\left(\frac{V^2}{s^2}\right)$ is the change in angular velocity since the addition of the previous lap. This equation requires two boundary conditions for each accretive solution. The core boundary condition has become:

$$\left.\frac{d(\delta P)}{dr}\right|_{r=1}=\left(\frac{E_\theta}{E_c}-1+\nu_{r\theta}\right)\left.\delta P\right|_{r=1}+\rho\delta\left(\frac{V^2}{s^2}\right) \qquad \{60\}$$

The outer lap boundary condition is modified as:

$$\delta P|_{r=s}=\frac{T_w|_{r=s}}{s}h-\rho V^2\left(\frac{h}{s}\right) \qquad \{61\}$$

Olsen formed these equations in terms of the difference in pressure (δP) rather than the difference in radial stress ($\delta\sigma_r$). Each lap which is added requires another solution of expression {59} and after that solution for the total pressure (P) must be updated (similar to expression {16}) such that the radial modulus (E_r) can be updated throughout the roll as a function of the total pressure. The output of this model is the pressure as a function of radius throughout the wound roll as a function of winding tension profile and wound roll velocity. Olsen presents results for newsprint wound at a winding tension (T_w) of 3000 KPa that indicate the average roll pressure drops from 70 to 42 KPa for a roll wound at slow speed versus one wound at 2000 m/min.

SUMMARY OF WINDING MODEL ABILITIES

The fundamental outputs from the various winding models in the literature are internal stresses within the roll. Plane stress models provide radial and circumferential stresses as a function of radius as outputs. Plane strain models provide radial, circumferential, and axial stresses as a function of radius as outputs. The first two dimensional models provided radial and circumferential stresses as a function of radius and discrete cross machine direction position as outputs. Many of these models can also be configured to provide deformations as outputs which in the case of two dimensional models allow the radial profile of various layers within the wound roll to be charted as a function of cross machine direction location. This can be interesting when winding webs of non-uniform thickness. Axisymmetric two dimensional models are based upon the finite element method. Deformations are the primary output from which radial (r), circumferential (θ), axial (z) stresses and shear stresses in the r-z plane as a function of radial and axial position can be calculated. It has been shown that time, temperature, and air entrainment can have substantial impact on these stress levels.

WOUND ROLL DEFECTS

Winding models would have little or no purpose if they could not be used to predict wound roll defects. As the models have increased in complexity the ability to predict more defects has become possible. There are not many references in the literature which focus on wound roll defects and fewer still which attempt to relate those defects to wound roll models. A good reference for roll defects in the paper industry has been compiled by

Smith [17]. This reference provides pictures and qualitative causes of various defects in paper rolls. Roisum [70] and Frye[71] both list a good number of wound roll defects as well. The following is a discussion of wound roll defects that can and cannot be attacked through the use of wound roll models.

Winding Defects that Can be Predicted with Wound Roll Models

Pressure Related Defects Many webs, either coated or uncoated, may wring or bond to the next layer in the winding roll when subjected to sufficient pressure. The bond which is formed can be so substantial that the web may tear or burst during subsequent unwinding operations. The force required to separate two layers of web can be calculated with knowledge of the surface energies of those surfaces in contact [72]. When the surface energies are unknown stacks of web material can be compressed in material testing systems which can subject the stack to a user defined pressure. The pressure can be increased until the pressure which will cause the layers to bond together can be found. Winding models can then be used to explore what winding conditions should be avoided to prevent pressures of that magnitude from existing in the wound roll. In Smith's reference [17] this type of defect is referred to as blocking. It might be argued that an experienced winding operator could solve blocking problems. There might be some truth to that notion, especially if the wound roll is in the *spongy* condition. A constant level of wound-on-tension produces pressures that are nearly constant over much of the wound roll radius, refer to Figure 4. Note as well in Figure 4 that the pressure nearly doubles in the vicinity of the core. Thus the operator may be able to prevent blocking over much of the radius of the wound roll by adjusting winding tension or nip load, but in the vicinity of the core he may have still have blocking. Converters don't wish to find the material in the vicinity of the core cannot be used and thus the winder parameters may require careful selection such that (1) blocking is avoided throughout the roll and (2) the roll can be unwound without internal slippage occurring, which will be addressed later. If the rolls being wound are fully compressed the problem becomes a greater challenge. A tapered tension profile with radius may need determined which prevents blocking throughout the roll while still giving the roll enough integrity that it can be shipped and handled.

Softness is a mark of quality in paper tissue. When subjected to the pressure within the wound roll, the tissue will compress and the softness will decrease. The pressure in a roll of tissue decayed 50% after 1000 minutes of storage shown in Figure 35. During that period the web was compacting in the radial direction and losing part of the web loft and softness. Struik [15] wound pieces of tissue into rolls of plastic film as a means of pressure measurement. He formed a calibration curve of pressure versus compaction and would recover the tissue samples during unwinding and infer the maximum pressure the tissue had been subjected to in the wound roll. By winding in tissue samples at various wound roll radii he was able to profile pressure versus wound roll radius. Thus wound roll pressure causes a loss of quality in tissue rolls but sufficient pressure must be retained to give the master or converted rolls sufficient integrity that they can be handled and shipped. What pressure decay and loss of loft will a tissue roll witness after 2 weeks, 4 weeks, or 2 months in storage? Viscoelastic winding models are a convenient means of solving this class of problem.

Bursts, Baggy Lanes, Ridges and Hardstreaks Bursts in paper are the result of tensile or shearing stresses in excess of the strength of the paper web. The strength of the web may be impacted by several inputs involved with the formation and the slitting of the web. It is sufficient to say that every web has an inherent tensile strength that can be

determined statistically through testing. It would seem obvious then that if the circumferential stresses due to winding are not allowed to exceed the tensile strength of the web that bursts should not occur. In fact bursts do occur at the winder and we must resolve how then in winding are stresses exerted in excess of the tensile strength which results in a burst or tensile failure of the web? Bursts are some of the most irritating problems a winder operator may have to solve because bursts commonly stop production or at least winding until the web can be rethreaded and spliced.

In center winding without a nip the one dimensional winding models produce the highest circumferential stresses exist near the core and the outer layer of the wound roll, refer to Figures 4 and 5. In this type of winder these tensile stresses cannot exceed the web line stress upstream of the winder and thus bursts would be as likely in the free span prior to the winder as on the winder itself. In other winder types this may not be the case. When center winding with an undriven nip, for instance, it was shown how the radial pressures in the wound roll increase with larger WOT which was the result of increased nip load, refer to Figures 19, 20, and 21. Now the maximum circumferential stresses in the outer layer of the winding roll will be larger than the stresses due to web tension and bursts will likely appear first on the winder. A winder operator may find that either nip load or web tension may be reduced to help solve a burst problem at the winder. If the operator decreased bursts by reducing nip load, he may not understand that the internal pressures in the roll have decreased significantly because he is now entraining more air than he was at the higher nip load that caused the bursts.

One of the dangers of drawing conclusions based only upon one-dimensional winding models is that the web variability across the width is ignored. Results from the two dimensional model shown in Figure 16 indicate the circumferential stresses at the web edges are over twice as large as those at the web center for a web whose thickness variation was shown in Figure 14. The large circumferential stress in combination with a slit edge that can vary in quality due to wear of slitter blades can increase the propensity for bursts. Thus two dimensional models can be powerful analysis tools for investigating what web thickness variation will lead to wound roll circumferential stresses that may exceed the tensile strength of the web and cause center or edge bursts to occur. A picture of a typical edge burst is shown in Figure 42.

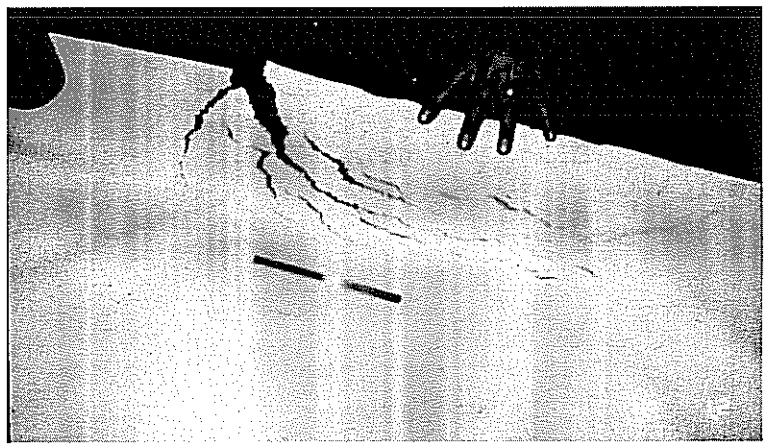

Figure 42 – Example of an Edge Burst in a Paper Web

Many plastic webs and some paper webs may elongate elastically or inelastically rather than burst. The circumferential stresses which were noted in Figure 16 could produce a web with permanently elongated or baggy edges if those stresses were sufficient to induce inelastic deformation or if the web is viscoelastic it would elongate more in the regions where the stresses were highest. Had the largest web thickness occurred closer to the center of the web, the circumferential stresses would have been locally higher in that region or "lane" and bagginess could have been expected in that location when unwinding. Thus two-dimensional wound roll models and visoelastic models are valuable tools for studying bursts and baggy lanes.

Cross machine direction locations with high web thickness also have locally high radial pressures, as shown in Figure 15. These locations will have a higher radial modulus that will be detectable with hardness testers such as the Beloit Rho Meter or the Paro Tester. This may locally form a defect called a *hardstreak* that runs circumferentially about the roll which may be accompanied by blocking since the radial pressure is locally high. In some cases the locally increased thickness will result in a ridge or a raised region that runs circumferentially about the roll. *Ridges* may or may not result in defects. The ridge may grow with wound roll diameter until the majority of the wound-on-tension focused on that CMD location and may finally result in a burst. Both hardstreaks and ridges can be analyzed with two-dimensional wound roll models. Examples of ridges which formed due to minor thickness variations are shown in Figure 43. The ridges are apparent in the line of reflected light.

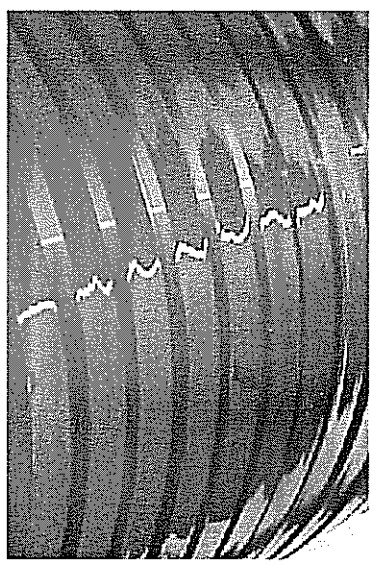

Figure 43 – Ridges on Rolls 12.7 mm wide Wound from 8.9 μm Polyester Film.

Wound roll models and viscoelastic roll models are useful in studying these types of defects from two perspectives. First, the models can be used to determine if an existing web thickness variation will cause defects and if other winder operating parameters would eliminate or produce less defects. Second, the models can be used to establish limits on thickness variation that will not produce defects under a range of winder operating parameters. The second perspective is valuable only if the process by which the web is made and coated can be adjusted to provide a web whose thickness variation is within the limits.

Slippage Related Defects Slippage within the wound roll is often considered a defect by those who must address the quality of the surface finish of a web. Slippage and bursts can be interrelated as slippage within a unwinding or winding roll can produce upsets in web tension that occur so rapidly that tension control systems cannot eliminate them. Often the slippage results in the abrasion of coated surfaces and a loss of quality if the abrasion has resulted in damage of the coated web surface. The slippage can in some cases be modeled with a parameter called the torque capacity of the roll. The torque capacity is the torque that can be applied to either a winding or unwinding roll just prior to slippage occurring between the web layers at some radial location [73]. Wound roll models provide an estimate of the radial pressure as a function of wound roll radius from one-dimensional models and also as a function of lateral location in the case of two-dimensional models. The torque capacity can be calculated using the expression:

$$T_{cap} = 2\pi\mu_{w/w} P r^2 W \qquad \{62\}$$

where $\mu_{w/w}$ is the friction coefficient between web layers, P is the radial pressure ($-\sigma_r$) at the radial location r and W is the web width. Slippage will occur whenever the applied torque to the roll exceeds the minimum value of the torque capacity within the wound roll. It should be noted that the web/web friction coefficient can be reduced by entrained air within the wound roll. When center winding a web without a nip or rider roll the radial pressure beneath the outer layer can be calculated using expression {12}:

$$P = \frac{T_w}{s} h \qquad \{63\}$$

where s is the radial location of the interface beneath the current outer layer. The torque capacity beneath the outer layer is thus:

$$T_{cap} = 2\pi\mu_{w/w} T_w h s W \qquad \{64\}$$

The applied torque to a center winding roll is:

$$T_{applied} = T_w h W s \qquad \{65\}$$

Again slippage will begin whenever the applied torque meets or exceeds the torque capacity. If expressions {64} and {65} are equated it is evident that whenever:

$$\mu_{w/w} \le \frac{1}{2\pi} \approx .159 \qquad \{66\}$$

that slippage will occur beneath the outer layer of the center winding roll. Thus it would appear difficult or impossible to wind low coefficient of friction materials with a center winder. Once slippage begins its direction can depend on web nonuniformity. The applied torque and torque capacities discussed would appear to relate to slippage that would vest itself in circumferential relative motion between web layers. The reality is that web nonuniformity across the web width causes lateral web forces as well such that circumferential slippage is often accompanied by lateral slippage which can result in edge offsets on the roll ends or in extreme cases can result in telescopes.

The ability of a wound roll model and expressions {62} and {65} to predict slippage will be demonstrated. A newsprint web, with the properties given in Table 6, is being center wound at a winding tension of 3.65 MPa. After the roll has wound for some period the winding tension drops to 0.41 MPa, possibly due to a splice, and winding continued. Later the winding tension returns quickly to the original level of 3.65 MPa. The winding tension profile, as a function of radius, and the circumferential stresses produced by a wound roll model are shown in Figure 44. The circumferential stresses are shown for two wound roll radii, just before the winding tension returned to 3.65 MPa and after the roll completed winding. Note that a significant negative circumferential stress

results from the return of full winding tension. The radial pressures predicted by the model are shown in Figure 45, note the decreased radial pressure when the roll had wound to 11.8 cm of radius compared to the pressures that existed as the roll completed winding at a radius of 14.3 cm. The applied torque and the torque capacity at both 11.8 and 14.3 cm of winding radius are shown in Figure 46. The applied torque is almost not visible in Figure 45, thus the gray region in Figure 46 was enlarged to produce Figure 47. Note when the roll has wound to a radius of 11.8 cm and the web tension has just returned to 3.65 MPa, the applied torque is in excess of the torque capacity. This roll was wound in the laboratory and is shown in Figure 48. Note that the roll slipped per evidence given by the lateral offsets and the skewed J-Line. Note also that the roll formed a buckled defect, at the 10 o'clock position, which could have been anticipated from the high negative circumferential stresses shown in Figure 44. The roll is no longer round which would produce a dynamic component of winding tension as the roll completed winding which would also be present when unwound. The winding model could also be used to predict a winding tension profile where the return to the maximum winding tension of 3.65 MPa could have been occurred over a longer time period and the defects prevented [73].

Web Properties		Core Properties	
E_θ	1.67 GPa	E_c	33 GPa
$E_{r,stack}$	K_1=47.1 KPa	Winder Parameters	
	K_2=32.8	T_w	Refer to Figure 43
μ_k	0.2		

Table 6 – Data for Winding of the Newsprint in Figures 43-47.

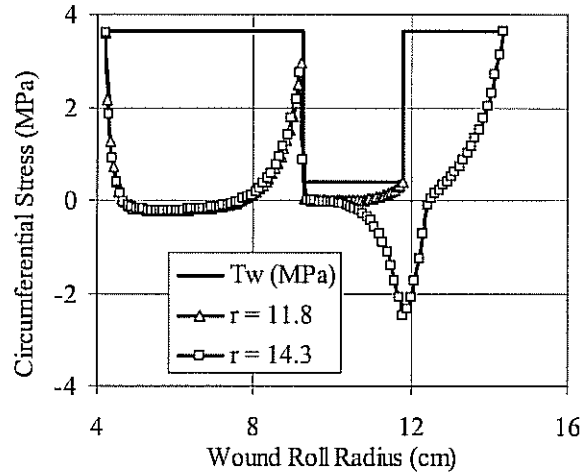

Figure 44 – Winding Tension & Circumferential Stresses in a Newsprint Roll.

Slippage may also appear at an unwinding roll. This may occur due to viscoelasticity and the decay of pressure throughout the wound roll. Thus a roll could be center wound and put in storage awaiting conversion. The roll could be retrieved but when placed on the unwinder, and perhaps unwound at the same tension at which it was wound, slippage could result. The viscoelastic tissue results shown in Figure 35 indicate half the pressure was lost from these rolls in the first 1000 minutes after winding. Per expression {62} half of the torque capacity has been lost during that time period as well

and thus these rolls cannot be unwound at the same tension at which they were wound without slippage resulting.

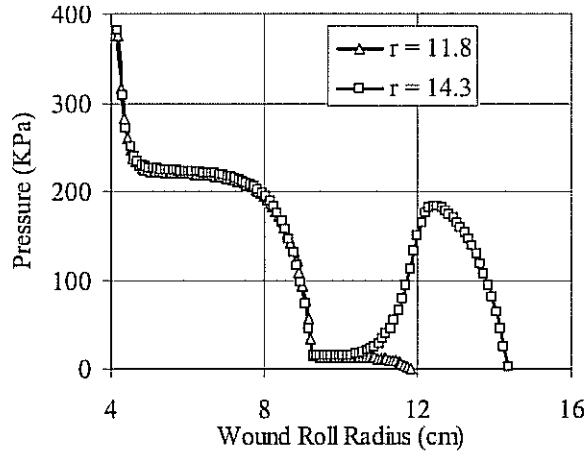

Figure 45 – Pressure in the Newsprint Roll.

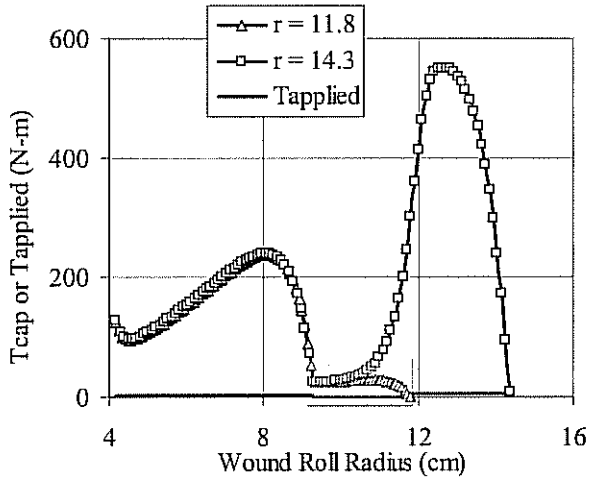

Figure 46 – Applied Torque and Torque Capacity in the Newsprint Roll.

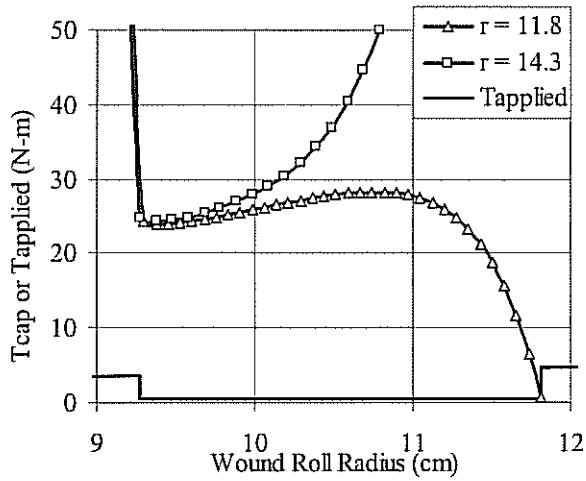

Figure 47 – Zoom of Figure 46, note the Applied Torque exceeds the Torque Capacity Immediately when the Winding Tension returns to 3.65 MPa.

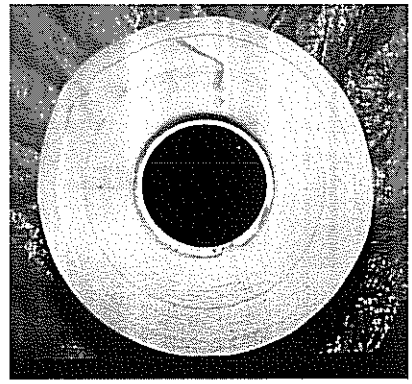

Figure 48 – Newsprint Roll Center Wound at the Winding Tension Profile shown in Figure 44.

The more common case is when a roll is wound in the presence of nip rollers either on a center winder with an undriven nip, a surface winder, a differential torque winder or a two drum winder. The nip forces provide local contact points that resist slippage. Then perhaps the roll is unwound on a center driven or braked unwind where it becomes subject to a higher applied torque in excess of the torque capacity that was wound into the roll and hence slippage results. This is a benefit of the belted unwinder in that the unwinding roll is subject to no torque under steady state conditions. However belted unwinders are notorious for allowing the unwinding roll to run ahead during deceleration causing loss of web tension, web breaks or crepe wrinkles [74]. An example of a wound roll that decelerated to quickly is shown in Figure 49. Note in the vicinity of the core that some compression or crepe wrinkles have formed.

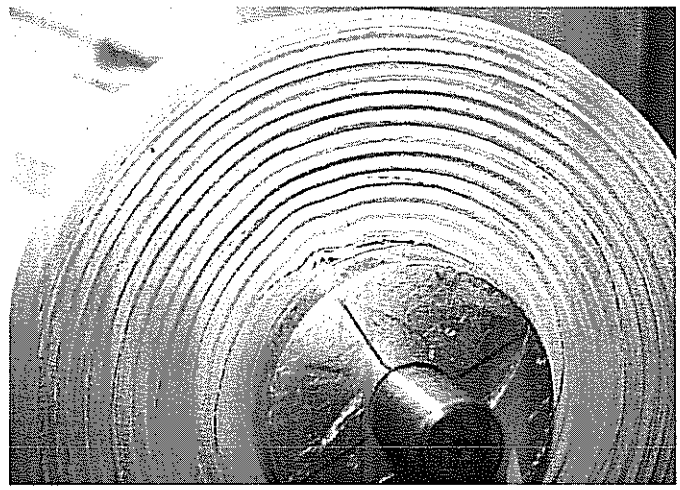

Figure 49 – Example of a Wound Roll Subjected to Inertial Torques in Excess of the Torque Capacity. Note the Spiral of the J-Line, which was a Radial Line Prior to Deceleration, and the Crepe Wrinkles near the Core.

Gross slippage may vest itself as a telescope defect in which the web may skate laterally off the end of the winding roll. In some cases gross slippage may also vest itself as a crepe wrinkle defect where a layer of web witnesses a local in-plane compression failure, refer to Figure 50. In this case the slippage is constrained to circumferential motion with little or no lateral slippage. A J-line struck at the edge of such a roll would exhibit instantaneous jumps at the radial locations where the crepe wrinkle occurred. In yet other cases the layer at which gross slippage is occurring may roll over upon itself and begin winding a miniature wound roll in between the adjacent layers. These defects are called cigars [17], an example of which is shown in Figure 51, in a tissue roll.

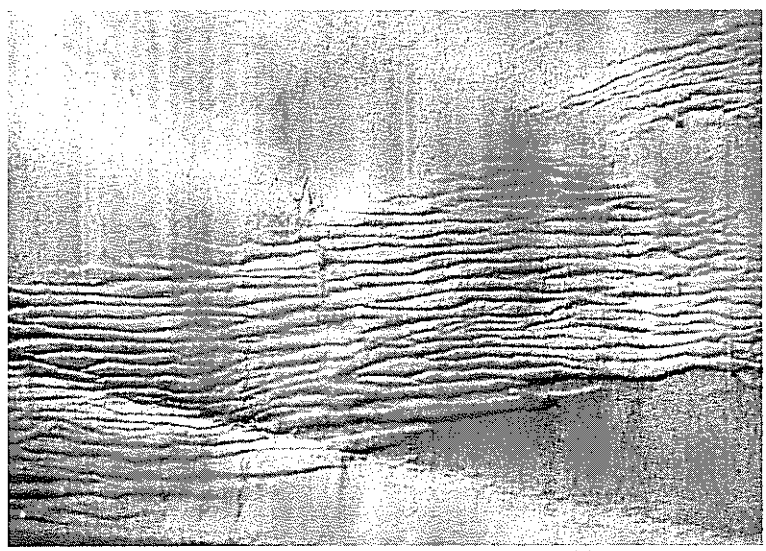

Figure 50 – Example of a Crepe Wrinkle

Figure 51 – A Cigar Defect.

All of these defects have one thing in common: In each case there was torque within the wound roll that exceeded the torque capacity. Thus had a roll been wound that had greater torque capacity these slippage related defects could have prevented. Often the torque capacity is minimal in the vicinity of splices due to the wound-on-tension dropping to a low level during splice operations. Lucas advocated retracting the rider roll on a two drum winder during web breaks to prevent or reduce crepe wrinkles [75] to reduce the forces that caused slippage within the wound roll whilst the torque capacity was low. In-roll slippage was the focus of a study by Vaidyanathan [76] in which he studied both the forces and torques within wound rolls that would induce slippage due to rolling resistance and deceleration.

Another slippage related defect is known as dishing. This defect is noted at the ends of a wound roll and appears as a lateral shifting of the layers in the wound roll. The edge of the web appears on track at the core, and at the outside of the winding roll, but the layers in between have shifted laterally usually but not always in one direction. This is not a web guiding issue, the outer layer of the winding roll is always at the guide point throughout the winding process. Thus the lateral slippage must occur for each layer after has been wound down into the roll. An example of a dish is shown in Figure 52. Cole [77] addressed this by studying the lateral forces and slippage that are developed by winding non-uniform thickness webs. Lucas [78] addressed the problem of dishing by studying the lateral or thrust forces that can be developed in various types of winding machinery. In these cases the outer layer may drift from the guide point depending on how the winding machinery is exerting the thrust load.

Telescoping defects differ from dishing defects. When a roll telescopes it is the result of loss of control of the lateral position of the outer layers of the winding roll. Often the web drifts laterally until it interferes with the machine which results in a web break. Telescope defects are often the result of a low friction coefficient between the web layers. Earlier it was shown that center winding becomes impossible when the friction coefficient becomes less than 0.159, expressions {64-66}. Some webs have friction coefficients less than 0.159, those webs must be wound on winders that subject the wound roll to less applied torque than a center winder.

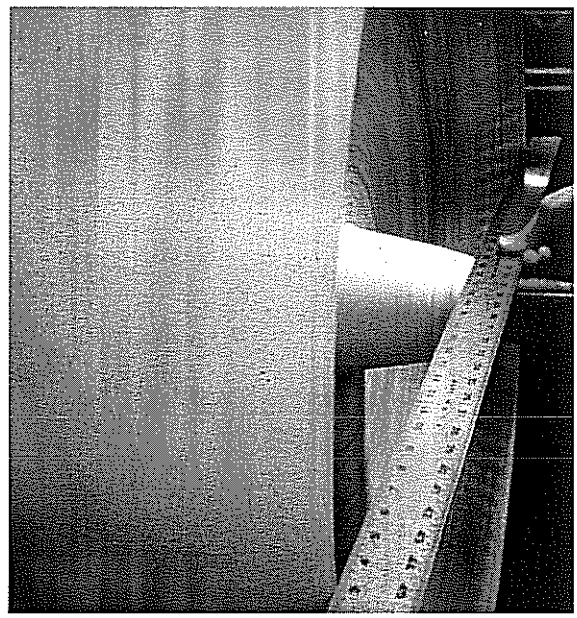

Figure 52 – A Dish Defect (note the outer layer aligns with the first layer on the core).

Air entrainment can decrease the effective friction coefficient to yet lower values. A simple friction relationship [79] that has been previously proven to be effective is:

$$\mu_t = \mu_{static} \quad \text{when } h_o \le R_{q,eq}$$

$$\mu_t = -\frac{\mu_{static}}{2R_{q,eq}} h_o + \frac{3}{2}\mu_{st} \quad \text{when} R_{q,eq} \le h_o \le 3R_{q,eq} \qquad \{67\}$$

$$\mu_t = 0 \quad \text{when } h_o \ge 3R_{q,eq}$$

where μ_t is defined as the effective friction or equivalently the amount the static friction coefficient has been depleted by entrained air. The equivalent roughness ($R_{q,eq}$) was previously defined in expression {58}. Using expression {67} one can determine the air layer thickness at which the effective friction coefficient will become 0.159 and gross slippage can be expected. One can also determine the air film thickness at which the traction decays to zero. When the traction decays to zero no contact exists between the outer layer of the winding roll and the layer beneath and telescoping becomes inevitable. Once the air film thickness is known, per expression {52} or {54} depending on the winder type, the winder operating parameters can be determined that will result in gross slippage or to telescoping. Air entrainment problems are usually not difficult to diagnose. Good quality rolls will be wound up to a certain wound roll radius and then layers will begin to drift or shoot out the roll end. Many rolls are wound at nearly constant tension and velocity. Per expression {52} it should be noted the air film thickness will increase proportionately as a function of wound roll radius. Thus each time a roll is wound, if the winder operating parameters remain unchanged, the wound roll will telescope at the same wound roll radius. Expressions {52}, {54} and {67} are valuable in that they can be used to determine if web tension, nip or rider load, final wound roll radius, or possibly surface roughness must be altered to prevent the problem.

Buckling and Instability Defects The potential for generating negative circumferential stress in wound rolls was shown in Figures 5 and 7. Many rolls are wound with negative circumferential stresses. A single web layer can withstand very little in-plane compressive stress prior to buckling. A web wound into a roll gains additional stability due to the surrounding web that is subject to radial pressure, similar to the stability gained by a beam when supported by an elastic foundation. Lee [80] studied winding conditions and compressive failure modes within a wound roll using wound roll models and failure models he developed for circumferential buckles in wound rolls. Lee found that in many cases a destabilizing effect on the wound roll was required to generate the circumferential buckles in addition to negative circumferential stresses in excess of the buckling stress. Thus the winding roll might appear of good quality during winding but if left in contact with a rider roller after the end of the roll was wound buckles would appear. This is similar to the starring defect which is described by Frye in which a wound roll stars or buckles after being subjected to an impact after winding [71]. Star defects are most common on rolls wound on two drum winders in cases where the majority of the roll was wound (probably erroneously) at a low WOT compared the WOT used as the roll was finished. Had this occurred on a center winder a buckling defect and a good deal of internal slippage similar to the wound roll shown in Figure 48 would occur due to the applied torque being in excess of the torque capacity of the wound roll. Two drum winders apply no steady state torque to the body of the roll (since the core is not braked or powered) which allows large changes in WOT to occur without inducing internal slippage. In the scenario discussed, large negative circumferential stresses may exist in the region of the roll beneath the radius where the WOT increased. At the completion of winding the roll may appear of good quality but impacts due to handling or line load support during roll storage can perturb the roll sufficiently to cause the star defect to occur, refer to Figure 53.

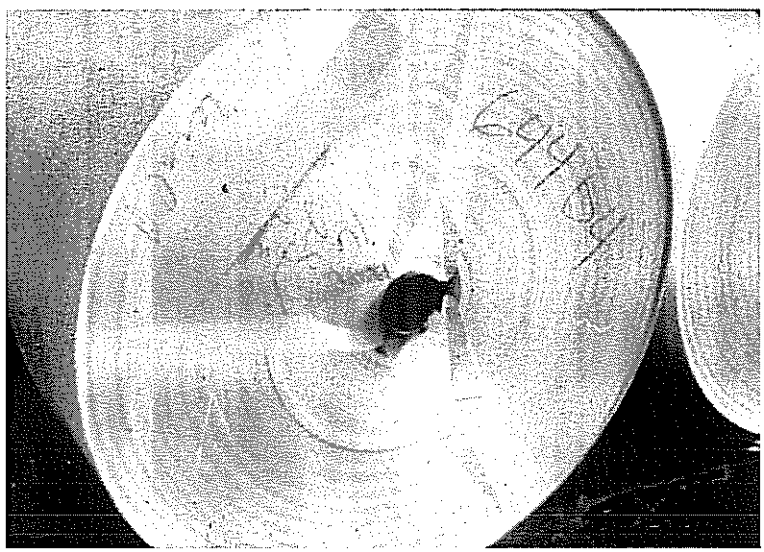

Figure 53 – A Star Defect.

Forrest [81] studied circumferential and axial buckles in wound rolls which he called corrugations using a plane strain winding model that accounted for entrained air. The entrained air decreases the effective foundation stiffness and increases the potential for

individual layers to buckle. Forrest hypothesized that the axial buckles were the result of negative axial stresses as were shown earlier in Figure 12. In some cases buckles appear later after a roll is wound and can be attributed to air escaping from the wound roll. We have wound roll models that account for air escape but currently they have not been used to study buckled roll defects [64-66]. Examples of circumferential and axial buckles are shown in wound rolls of polyester in Figure 54 and 55, respectively.

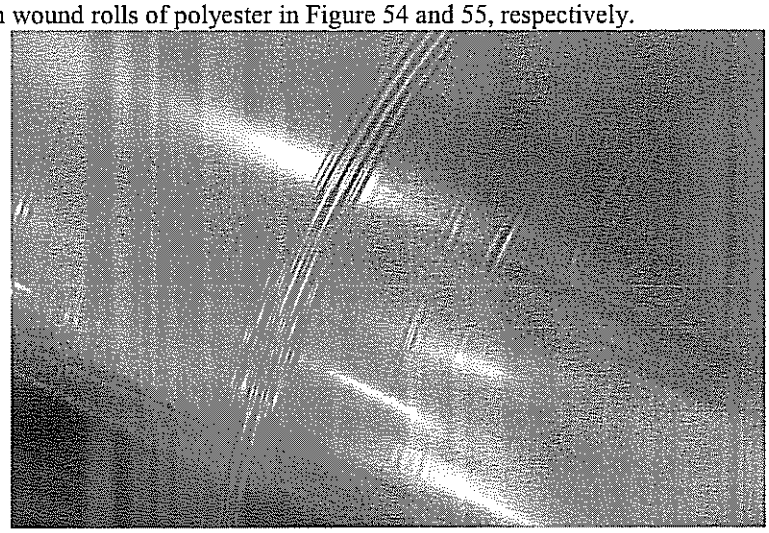

Figure 54 – Circumferential Corrugations in a Wound Roll of Polyester

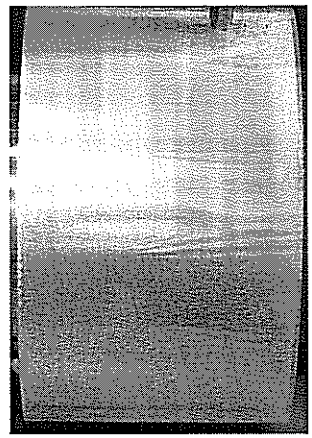

Figure 55 – Axial Corrugations in a Wound Roll of Polyester.

Core Failure and Loose Cores If the winder core shaft cannot be inserted into a failed core or if unwind tension cannot be developed due to a loose core entire loss of a wound roll can result. Entire wound rolls can become scrap as a result of core problems. In some cases the winding pressures are so substantial that the core may fail. Core failure can either be a structural failure of the core, sometimes a local buckle in the core wall, or if the core stiffness is insufficient negative circumferential stresses can result in the web layers in the vicinity of the core [82] and cause those layers to buckle as discussed in the previous paragraph.

Although wound roll models can be used to study core failures, both the core stiffness and the core strength are needed to determine when core failures will occur. The core stiffness is determined by measuring the radial deformation of the core using strain gages or laser displacement gages whilst the core is subjected to an external pressure. The core strength can be determined by increasing the external pressure until failure occurs. This requires a barometric or a hydraulic compression test chamber in which the exterior of the core can be subjected to pressure while the interior is subject only to atmospheric pressure, refer to Figure 56[83-86].

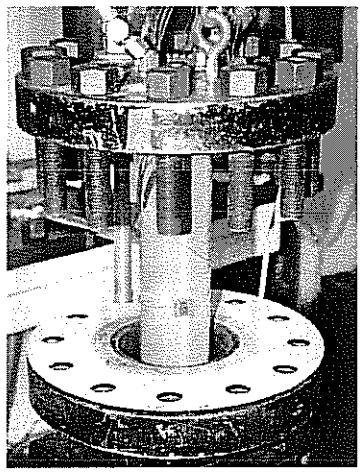

Figure 56 – Pressure Chamber for determining the Stiffness and Strength of a Core (note the strain gage attached to the core).

Given the core stiffness (E_c) and the web material and winder operating parameters wound roll models can be used to determine if core failures are to be expected. Perhaps an alternative perspective is that the wound roll model can aid in the decision process of what core material and dimensions are needed to prevent core failures when the winder operating and web material parameters are given.

As an example the rolls of fine paper which were wound earlier in the *spongy* state will used again, refer to Figures 4 and 5. In that example the fine paper was wound on a high stiffness metal core, whose stiffness was 1.9 GPa. The effect of core stiffness is shown in Figures 57 and 58 on the pressures and circumferential stresses, respectively.

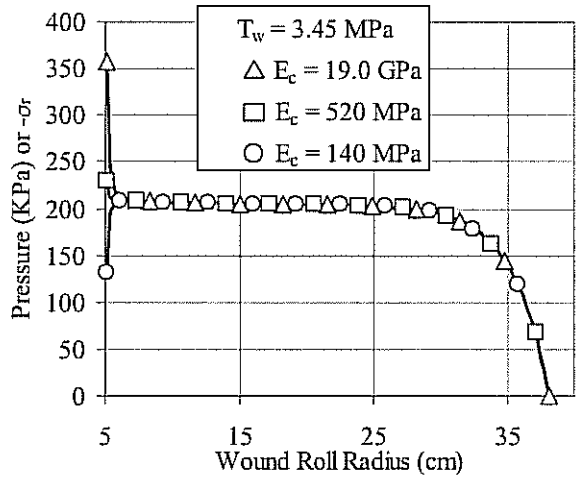

Figure 57 – Pressure in Rolls of Fine Paper as a Function of Core Stiffness.

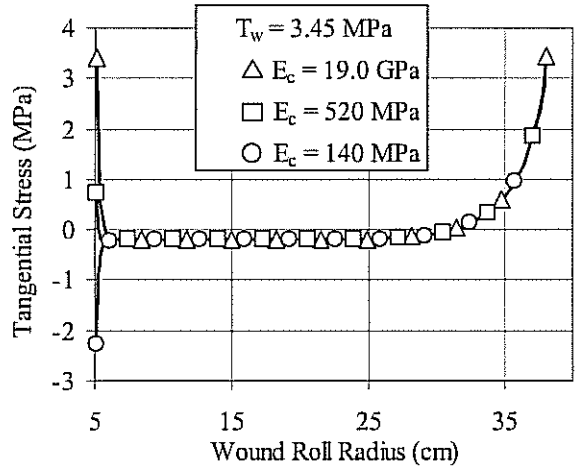

Figure 58 – Circumferential Stress in Rolls of Fine Paper as a Function of Core Stiffness.

Note for a wound roll in the *spongy* state that only the pressures and circumferential stresses in the vicinity of the core are affected by the core stiffness. Note how the pressure has dropped in the vicinity of the core with the least stiffness. This will result in a low torque capacity next to the core and may be responsible for loss of the entire roll depending on the unwind torque in the next process. The other two core stiffness values are representative of fiber cores. Note the large negative circumferential stresses in Figure 58 for the least core stiffness that could cause axial buckles. The fiber core with a stiffness of 520 MPa appears just adequate to maintain a pressure comparable to that out in the roll body and to prevent negative circumferential stresses at the core. Cores are often not returned by converters to those who produce webs, and thus it is desirable to have the core cost at little as possible. There is a direct correlation between core stiffness and core cost, thus the wound roll model can be a powerful tool to aid in the selection of a core which is just adequate for winding a particular product under specific conditions.

Winding versus Unwinding Defects Defects often are witnessed when unwinding a roll that were not seen when the roll was previously wound. This can be due to the

winder being configured differently than the unwinder. For instance, a roll may have been wound on a two drum winder where the winding roll was subject to little torque between the core and the outside of the wound roll except for the inertial torques due to acceleration and deceleration. Also the drums of the two drum winder provide distributed support of the wound roll across the roll width. In the next operation the wound roll may be unwound on an unwinder that provides a braking torque to the core of the wound roll which for convenience may be supported on stub shafts. Thus the wound roll which appeared to wind nicely may behave badly in the unwinder where it was first subjected to significant torque. Also the core and web outside the core may suffer badly due to the stub shafts. With the entire weight of the roll supported on two stub shafts the internal nip load can be very high. The associated nip induced slippage has been known to cause web fracture failures and crepe wrinkles inside the wound roll just outside the cores in the region of the core that is supported by the stub shafts, refer to Figure 59. Lucas [87] denoted this phenomenon as "gearing." Innala and Vanninen [88] analyzed the stresses at roll edges and found they could be sufficient to fail the web.

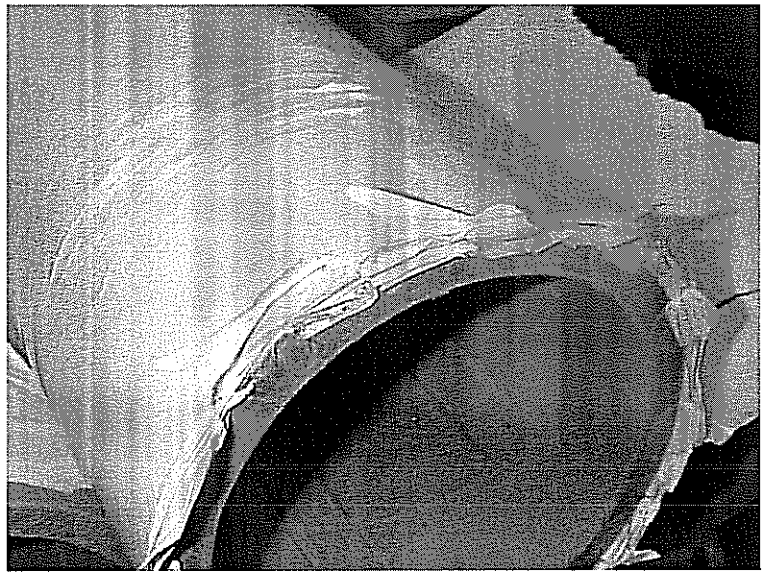

Figure 59 – Paper Failure above Stub Shafts in an Unwinder *(Printed with the permission of L.G. Eriksson).*

Wound rolls are often not stored in the best of conditions and then not converted expediently. Thermoelasticity and viscoelasticity have been discussed and shown to significantly affect the stresses within the wound roll. Thus a roll wound on a center winder at a given web tension should not be expected to unwind at the same tension on a braked center unwinder if the storage time has been significant. What storage time is significant will be dependent on the particular web properties and the storage conditions. This is an excellent example of how useful wound roll models can be when they are used to predict allowable conversion times of wound rolls with known internal stresses that must be stored in a given environment.

Winding Defects that Cannot be Predicted with Wound Roll Models

Defects that cannot currently be attacked are those that involve gross circumferential slippage. As an example winding models can predict the onset of slippage through the torque capacity calculation. Crepe wrinkles and cigars (Figures 50 and 51) are examples of defects where slippage has progressed much beyond the onset. It could be stated that crepe wrinkles and cigars could be prevented if no torque in excess of the torque capacity was input to the roll. The models cannot help us determine how large these defects will be and how much circumferential slippage will accompany the defects. This would also be true of web scratches. If no torque beyond the torque capacity was input to the roll there would be no scratching resulting due to winding the web. The models cannot predict how long the scratches will be if the applied torque is in excess of the torque capacity.

Similarly out-of-round rolls can not be predicted. In Figure 48 an out-of-round feature was generated as a result of gross circumferential slippage. Models cannot currently determine how much circumferential slippage was necessary to create that out-of-round feature nor can the models predict the magnitude of the out-of-round feature. Out-of-round rolls are of course unpopular at unwind stands where tension control is important. The out-of-round feature is responsible for a once per revolution tension disturbance who frequency increases as the unwinding roll diminishes at constant web velocity. Models do not currently exist which would predict the buckling of high aspect ratio wound rolls (where the width is small compared to the diameter of the wound roll).

CONCLUSION

It has been shown that the winding models are helpful in assessing how various web and winder parameters affect the internal stresses that are generated in winding or thereafter. Winder type, winder operating parameters including web tension, nip loads, drum torques, web material properties including the radial and circumferential moduli and the creep functions in the advent of viscoelasticity, storage environment, core stiffness and core size and final wound roll diameter, air entrainment, winder speed, and thickness variation have all been shown to impact the internal stresses. Quantitative WOT analysis is required to apply the roll models to various winder types. Although WOT models are evolving, research needs to continue in this area such that all winding with all winder types can be modeled.

Many winding defects can be studied with these models if those defects can be quantified in terms of internal stresses output by the model. It has been shown that pressure related defects, bursts, baggy lanes, ridges, hard streaks, slippage related defects, buckling and instability defects, core loss and core slippage defects can be studied using these models.

What does the future hold for this topic? For winding models to apply to all winders we must develop better analytical models for the estimation of wound-on-tension for single and multiple drum winders. Techniques are needed that can account for the complexity of the wound roll properties in addition to the compressibility of the roll covers which are now being employed. Winding models need to progress beyond one and two dimensions if we hope to model defects where there is gross circumferential slippage. Winding defect models need further development and verification.

Even with these shortcomings the current winding and defect models can be put to good use. Several examples have been provided herein showing what defects can be

predicted through the use of wound roll and defect models. Certainly there are great gains that could be made with current models. The fine coated paper web 1.5% thicker at the edges with circumferential stresses twice as large at the edges compared the center is a good example. This is an instance were those involved in forming the web can be given practical limits for thickness variation to prevent bursts at winders through use of the models.

ACKNOWLEDGEMENTS

The author would like to thank the Program Committee of the International Conference on Web Handling for inviting him to write this keynote paper on a topic which has held great interest for him. The author would also like to thank the sponsors of the Web Handling Research Center, Oklahoma State University, and the State of Oklahoma for the financial support which has allowed him to allocate time to write this review. The author would like to thank Beloit Corporation, who was once a sponsor of the Web Handling Research Center, and gave him permission to copy and use the photographs seen in Figures 42, 50, 52, and 53. He would also like to thank Leif Eriksson for allowing him to include the reprints of the WOT measurements for single and two drum winders shown in Figures 18 and 26 as well as the "gearing" failure shown in Figure 59.

REFERENCES

1. Gutterman, R. P. "Theoretical and Practical Studies of Magnetic Tape Winding Tensions and of Environmental Roll Stability," US Contract No. DA-18-119-SC-42, 1959.
2. Catlow, M. G. and Walls, G. W. "A Study of Stress Distribution in Pirns," Journal of Textile Institute Part 3, pp. T410-429, 1962.
3. Altmann, H. C. "Formulas for Computing the Stresses in Center-Wound Rolls," Tappi Journal, vol. 51, no. 4, pp. 176-179, April 1968.
4. Yagoda, H. P. "Integral Formulas for Wound Rolls," Mechanics Research Communications, vol. 7, no. 2, 1980, pp. 103-112.
5. Boutaghou, Z.E. and Chase, T.R., "Formulas for Generating Prescribed Residual Stress Distributions in Center Wound Rolls," ASME Journal of Applied Mechanics, V. 58, September 1991, pp. 836-84.
6. Pfeiffer, J. D., "Internal Pressures in a Wound Roll," Tappi Journal, V. 49, No. 8, August 1966, pp. 342-347.
7. Hakiel, Z., "Nonlinear Model for Wound Roll Stresses," Tappi Journal, V. 70, No. 5, May 1987, pp. 113-117.
8. Willett, M.S., and Poesch, W. L., "Determining the Stress Distributions in Wound Reels of Magnetic Tape Using a Nonlinear Finite-Difference Approach," Journal of Applied Mechanics, V. 55, June 1988, pp. 365-371.
9. Benson, R.C., "A Nonlinear Wound Roll Model Allowing for Large Deformation," ASME Journal of Applied Mechanics, V. 62, December 1995, pp. 853-859.
10. Pfeiffer, J. D., "Prediction of Roll Defects from Roll Structure Formulas," Tappi Journal, V. 62, no. 10, October 197, pp. 83-85.
11. Pfeiffer, J.D., and Hamad, W.Y., "How Core Stiffness and Poisson Ratio Affect Energy Balance Roll Structure Formulas," Proceedings of the First International Conference on Web Handling, Web Handling Research Center, Oklahoma State University, 1991, pp. 1-16.
12. Burns, S.J., Meehan, R.R., and Lambroupoulos, J.C., "Strain-Based Formulas for Stresses in Profiled Center-Wound Rolls," TAPPI Journal, V. 82, No. 7, July 1999, pp. 159-167.
13. Hamad, W., Winding Mechanics of Anisotropic Materials, Pira International, 1998.
14. Zabaras, H., Liu, S., Koppuzha, J., Donaldson, E., "A Hypoelastic Model for Computing the Stresses in Center-Wound Rolls of Magnetic Tape," ASME Journal of Applied Mechanics, Vol. 61, 1994, pp. 290-295.
15. Struik, L., "Lecture Notes on Winding Studies Presentation," TNO Rubber Institute, Delft, Netherlands, 1984.
16. Good, J.K., Pfeiffer, J.D., and Giachetto, R.M., "Losses in Wound-On-Tension in the Center Winding of Wound Rolls," Proceedings of the Web Handling Symposium, ASME Applied Mechanics Division, AMD-Vol. 149, 1992, pp. 1-12.
17. Smith, D.R., Roll and Web Defect Terminology, TAPPI Press, 1992.
18. Kedl, D.M., "Using a Two Dimensional Winding Model to Predict Wound Roll Stresses that Occur due to Circumferential Steps in Core Diameter or to Cross Web Caliper Variation," Proceedings of the First International Conference on

Web Handling, Web Handling Research Center, Oklahoma State University, 1991, pp. 99-112.
19. Shelton, J.J., "Dynamics of Web Tension Control with Velocity or Torque Control," Proceedings of the American Control Conference, Seattle, WA, 1986, pp. 1423-1427.
20. Hakiel, Z., "On the Effect of Width Direction Thickness Variations in Wound Rolls," Proceedings of the First International Conference on Web Handling, Web Handling Research Center, Oklahoma State University, 1991, pp. 79-98.
21. Cole, K.A., and Hakiel, Z., "A Nonlinear Wound Roll Model Accounting for Widthwise Web Thickness Nonuniformities," Proceedings of the Web Handling Symposium, ASME Applied Mechanics Division, AMD-Vol. 149, 1992, pp. 13-24.
22. Hoffecker, P. and Good, J. K., "An Axisymmetric Finite Element Model for Center Winding Webs," Proceedings of the Eighth International Conference on Web Handling, Web Handling Research Center, Oklahoma State University, Stillwater, Oklahoma, 2005.
23. Lee, Y. M., and Wickert, J. A., "Stress Field in Finite Width Axisymmetric Wound Rolls," ASME Journal of Applied Mechanics, Vol 69, no 2, 2002, pp. 130-138.
24. Lee, Y. M., and Wickert, J. A., "Width-wise Variation of Magnetic Tape Pack Stresses," ASME Journal of Applied Mechanics, Vol 69, no 3, 2002, pp. 358-369.
25. Spitz, D. A., "Effects of Cross Direction Caliper Variations in Winding," TAPPI Journal, V. 52, No. 6, June, 1969, pp. 1168-1170.
26. Pfeiffer, J.D., "Internal Pressures in a Wound Roll of Paper," TAPPI Journal, V. 49, No. 8, August, 1966, pp. 342-347.
27. Pfeiffer, J.D., "Mechanics of a Rolling Nip on Paper Webs," TAPPI Journal, V. 51, No. 8, August, 1968, pp. 77A-85A.
28. Rand, T., and Ericsson, L.G., "Physical Properties of Newsprint Rolls during Winding," TAPPI Journal, V. 56, No. 6, June, 1973, pp. 153-156.
29. Pfeiffer, J.D., "Nip Forces and their Effect on Wound-In Tension," TAPPI Journal, V. 60, No. 2, February, 1977, pp. 115-117.
30. Pfeiffer, J.D., "Wound-Off Tension Measurement in Paper Rolls," TAPPI Journal, V. 60, No. 3, March, 1977, pp. 106-108.
31. Good, J.K., and Fikes, M.W.R., "Predicting the Internal Stresses in Center-wound Rolls with an Undriven Nip Roller", TAPPI Journal, V. 74, No. 6, June, 1991, pp. 101-109.
32. Good, J.K., and Wu, Z., "The Mechanism of Nip Induced Tension in Wound Rolls," ASME Journal of Applied Mechanics, Vol. 60, No. 4, 1993, pp. 942-947.
33. Good, J.K., Wu, Z., and Fikes, M.W.R., "The Internal Stresses in Wound Rolls with the Presence of a Nip Roller," ASME Journal of Applied Mechanics, Vol.61, No.1, March, 1994.
34. Johnson, K.L., Contact Mechanics, Cambridge University Press, p. 312, 1985
35. Steves, R.E., "The Effect of Nip Load on Wound-On-Tension in Surface Winding," M.S. Thesis, Oklahoma State University, May, 1995.
36. Good, J.K., Hartwig, J., and Markum, R., "A Comparison of Center and Surface Winding Using the Wound-In-Tension Method," Proceedings of the

Fifth International Conference on Web Handling, Web Handling Research Center, Oklahoma State University, Stillwater, Oklahoma, 1999, pp. 87-104.
37. Welp, E.G., and Guldenberg, B., "Analysis of the Kinematic and Dynamic Process during Winding based on a Systematology of Models for Winding Mechanics," Proceedings of the Fourth International Conference on Web Handling, Web Handling Research Center, Oklahoma State University, Stillwater, Oklahoma, 1997, pp. 71-89.
38. Jorkama, M., and von Hertzen, R., "Contact Mechanical Approach to the Winding Nip," Proceedings of the Fifth International Conference on Web Handling. Web Handling Research Center, Oklahoma State University, Stillwater, Oklahoma, 1999,pp. 39-49.
39. Jorkama, M., and von Hertzen, R., "Development of Web Tension in a Winding Nip," Proceedings of the Sixth International Conference on Web Handling, Web Handling Research Center, Oklahoma State University, Stillwater, Oklahoma, 2001, pp. 123-134.
40. Jorkama, M., and von Hertzen, R., "The Mechanism of Nip Induced Tension in Winding," Journal of Pulp and Paper Science, V. 28, No. 8, August, 2002, pp.280-284.
41. Good, J.K., "Modeling Nip Induced Tension in Wound Rolls," Proceedings of the Sixth International Conference on Web Handling, Web Handling Research Center, Oklahoma State University, Stillwater, Oklahoma, 2001, pp. 103-122.
42. Olsen, J.E., and Irgens, F., "Aspects of Two Drum Winding," Proceedings of the Fourth International Conference on Web Handling, Web Handling Research Center, Oklahoma State University, Stillwater, Oklahoma, 1997, pp. 90-101.
43. Olsen, J.E., and Irgens, F., "Dynamic Analysis of Two Drum Winding," Journal of Pulp and Paper Science, V. 25, No. 8, August, 1999, pp. 278-282.
44. Good, J.K., Cowan, B.R., Dolezal, L.E., and Markum, R., "Wound-On-Tension for Two Drum Winders," Proceedings of the Seventh International Conference on Web Handling, Web Handling Research Center, Oklahoma State University, Stillwater, Oklahoma, 2003.
45. Tramposch, H., "Anisotropic Relaxation of Internal Forces in a Wound Reel of Magnetic Tape," Journal of Applied Mechanics, December 1967, pp. 888-894.
46. Connolly, D. and Winarski, D. J., "Stress Analysis of Wound Magnetic Tape," ASLE Special Publication SP-16, pp. 172-182.
47. Qualls, W.R., and Good, J.K., "Thermal Analysis of a Wound Roll," ASME Journal of Applied Mechanics, Vol. 64, No. 4, December, 1997, pp. 871-876.
48. Qualls, W.R., "Hygrothermomechanical Characterization of Viscoelastic Centerwound Rolls," PhD Dissertation, Oklahoma State University, May, 1995.
49. Tramposch, H., "Relaxation of Internal Forces in a Wound Reel of Magnetic Tape," Journal of Applied Mechanics, Volume 32, No. 4, December 1965, pp. 865-873.
50. Lin, J. Y. and Westmann, R. A., "Viscoelastic Winding Mechanics," ASME Journal of Applied Mechanics, Volume 56, December 1989, pp. 821-827.
51. Qualls, W.R., and Good, J.K., "An Orthotropic Viscoelastic Winding Model Including a Nonlinear Radial Stiffness," ASME Journal of Applied Mechanics, Vol. 64, No. 1, March, 1997, pp. 201-207.

52. Blok, H., and VanRossum, J.J., "The Foil Bearing – A New Departure in Hydrodynamic Lubrication," Lubrication Engineering, Vol. 9, 1953, pp. 316-320.
53. Knox, K.L., and Sweeney, T.L., "Fluid Effects Associated with Web Handling," Industrial Engineering Chemical Process Design Development, Vol. 10, no. 2, 1971, pp. 201-205.
54. Holmberg, M.W., and Good, J.K., "The Effect of Air Entrainment in Center Wound Rolls," Proceedings of the Second International Conference on Web Handling, Web Handling Research Center, Oklahoma State University, Stillwater, Oklahoma, 1993, pp. 246-264.
55. Taylor, R.M., and Good, J.K., "Entrained Air Films in Center Wound Rolls – With and Without the Nip," Proceedings of the Fourth International Conference on Web Handling, Web Handling Research Center, Oklahoma State University, Stillwater, Oklahoma, 1997, pp. 189-204.
56. Welp, E.G., Kleinert, A., and Schuler, D., "Prevention of Web Floating at Wrapped Transport and Guide Rollers," Proceedings of the Seventh International Conference on Web Handling, Web Handling Research Center, Oklahoma State University, Stillwater, Oklahoma, 2003.
57. Eshel, A., Baker, S., Hartman, A., and Orcutt, F.K., "Mechanical Aspects of Archival Storage of Magnetic Tape," Tribology and Mechanics of Magnetic Storage Systems, American Society of Lubrication Engineers Special Publication 16, 1984, pp. 148-157.
58. Chang, Y.B., Chambers, F.W., and Shelton, J.J., "Elastohydrodynamic Lubrication of Air Lubricated Rollers," ASME Journal of Tribology, Vol. 118, July, 1996, pp. 623-628.
59. Blevins, R.D., Applied Fluid Dynamics Handbook, Krieger, Malabar, Florida, 1992, pp. 502.
60. Keshavan, M.B., and Wickert, J.A., "Air Entrainment during Steady-State Winding," ASME Journal of Applied Mechanics, Vol. 64, 1997, pp. 916-922.
61. Good, J.K., and Covell, S.M., "Air Entrapment and Residual Stresses in Rolls Wound with a Rider Roll," Proceedings of the Third International Conference on Web Handling, Web Handling Research Center, Oklahoma State University, Stillwater, Oklahoma, 1995, pp. 95-112.
62. Bouquerel, F., and Bourgin, P., "Irreversible Loss of Foil Tension due to Aerodynamical Effects," Proceedings of the Second International Conference on Web Handling, Web Handling Research Center, Oklahoma State University, Stillwater, Oklahoma, 1993, pp. 265-285.
63. Forrest, A.W., "Wound Roll Stress Analysis Including Air Entrainment and the Formation of Wound Roll Defects," Proceedings of the Third International Conference on Web Handling, Web Handling Research Center, Oklahoma State University, Stillwater, Oklahoma, 1995, pp. 113-133.
64. Lei, H., Cole, K.A., and Weinstein, S.J., "Modeling Air Entrainment and Temperature Effects in Winding," ASME Journal of Applied Mechanics, Vol. 70, November, 2003, pp. 902-914.
65. Taylor, R.M., "Prediction of the Effects of Air Entrainment on Wound Roll Structure," PhD Dissertation, Oklahoma State University, 2000.
66. Tanimoto, K., "In-Roll Stress Analysis of Wound Roll with the Air Entrainment and the Permeation," Proceedings of the Sixth International Conference on Web Handling, Web Handling Research Center, Oklahoma State University, Stillwater, Oklahoma, 2001, pp. 63-78.

67. Yagoda, H.P., "Centrifugally-Induced Stresses within Center-Wound Rolls – Part I," Mechanics Research Communications, Vol. 7, no. 3, 1980, pp. 181-193.
68. Yagoda, H.P., "Centrifugally-Induced Stresses within Center-Wound Rolls – Part II," Mechanics Research Communications, Vol. 7, no. 4, 1980, pp. 233-240.
69. Olsen, J.E., "On the Effect of Centrifugal Force on Winding," TAPPI Journal, Vol. 78, No. 7, July, 1995, 191-195.
70. Roisum, D.R., The Mechanics of Winding, TAPPI Press, Atlanta, Georgia, 1994.
71. Frye, K.G., Winding, TAPPI Press, Atlanta, Georgia, 1990.
72. Johnson, K.L., Contact Mechanics, Cambridge University Press, 1989, p. 125.
73. Vaidyanathan, N., and Good, J.K., "The Importance of Torque Capacity in Predicting Crepe Wrinkles and Starring within Wound Rolls," Proceedings of the Third International Conference on Web Handling, Web Handling Research Center, Oklahoma State University, Stillwater, Oklahoma, 1995, pp. 134-155.
74. Hamel, J., Menard, A., and McDonald, D., "The Factors that Control Runahead on Printing Presses," Proceedings of the Fifth International Conference on Web Handling, Web Handling Research Center, Oklahoma State University, Stillwater, Oklahoma, pp. 297-312, 1999
75. Lucas, R.G., "Winder Crepe Wrinkles – Their Causes and Cures," Proceedings of the 1981 TAPPI Finishing and Converting Conference, TAPPI Press, Atlanta, Georgia, USA, 1981, pp. 91-98.
76. Vaidyanathan, N., "A Study of Wound Roll Slippage," PhD Dissertation, Oklahoma State University, 1991.
77. Cole, K.A., "A Model for the Prediction of Wound Roll Dishing," Proceedings of the Fourth International Conference on Web Handling, Web Handling Research Center, Oklahoma State University, Stillwater, Oklahoma, 1997.
78. Lucas, R.G., "Dishing in Winding Rolls of Paper," TAPPI Journal, July 1977.
79. Good, J.K., and Beisel, J.A., "Buckling of Orthotropic Webs in Process Machinery," Proceedings of the Seventh International Conference on Web Handling, Oklahoma State University, June 1-4, 2003.
80. Lee, B.O, "Buckling Analysis of Starred Roll Defects in Center Wound Rolls," PhD Dissertation, Oklahoma State University, 1991.
81. Forrest, A.W., "Wound Roll Stress Analysis including Air Entrainment and the Formation of Roll Defects," Proceedings of the Third International Conference on Web Handling, Oklahoma State University, June 18-21, 1995.
82. Yagoda, H.P., "Resolution of a Core Problem in Wound Rolls," ASME Journal of Applied Mechanics, Vol. 47, January, 1980, pp. 847-854.
83. Gerhardt, T.D., "External Pressure Loading of Spiral Paper Tubes: Theory and Experiment," ASME Journal of Engineering Materials and Technology, Vol.122, 1990, pp. 144-150.
84. Gerhardt, T.D, Qiu, Y.P., Johnson, C.G., and Rhodes, D.E., "Engineering Paper Tubes to Improve Winding Performance of Various Materials," Proceedings of the Fifth International Conference on Web Handling, Web Handling Research Center, Oklahoma State University, Stillwater, Oklahoma, 1999, pp. 251-264.
85. Gerhardt, T.D, Rhodes, D.E ., Johnson, C.G., Wang, Y., and McCarthy, M., "Performance of Paper Tubes," Proceedings of the Fifth International

Conference on Web Handling, Web Handling Research Center, Oklahoma State University, Stillwater, Oklahoma, 1999, pp. 265-278.
86. Henning, J.S., "Effects of Relaxation of a Core on a Wound Roll," MS Thesis, Oklahoma State University, 1997.
87. Lucas, R., "Internal Gearing in a Roll of Paper," TAPPI 1974 Finishing & Converting Conference Proceedings, TAPPI Press, Atlanta, Georgia.
88. Innala,M.,and Vanninen, R., "Experimental and Numerical Studies of the Reelspool and the Parent Roll Interaction under Gravity Forces," Proceedings of the Sixth International Conference on Web Handling, Oklahoma State University, June 10-13, 2001, pp. 145-158.

Keynote Presentation – *The Abilities & Inabilities of Wound Roll Models to Predict Defects*

J. K. Good, Oklahoma State University, USA

Name & Affiliation	**Question**
David Landskron Quad Graphics Printing	When you were confirming the air film thickness in winding rolls you used wax to seal the roll ends during winding to prevent air loss. The other day, someone said let's model what we can build, let's build what we can model. What if you put large pucks on the end of the roll and evacuated the entrained air through them. Would you actually be able to make a roll that didn't have the entrained air and then would that have some merit?
Name & Affiliation	**Answer**
Keith Good Oklahoma State University	There may be merit in exploring other means to prevent air from entraining into rolls. Currently we know that a well designed nip roll that does not bounce is very effective in reducing entrained air. The puck system you describe might allow rolls to be center wound at high speeds without using a nip roller. In extreme case is a vacuum coater where there is no air. That certainly gives you the baseline to start from. This problem is dependent on the roughness of the web; it is highly dependent on the width of the web. If I had had a winder as wide as a production winders, I wouldn't even have had to seal the edges because the rate at which air escapes from the edges of the roll is related to the inverse of width squared.